

The domino problem of the hyperbolic plane is undecidable, new proof

Maurice Margenstern

Laboratoire de Génie Informatique, de Production et de Maintenance, EA 3096,
 Université de Lorraine, Bâtiment A de l'UFR MIM,
 3 rue Augustin Fresnel,
 BP 45112,
 57073 Metz Cedex 03, France,
e-mail : maurice.margenstern@univ-lorraine.fr

Abstract

The present paper is a new version of the arXiv paper revisiting the proof given in a paper of the author published in 2008 proving that the general tiling problem of the hyperbolic plane is undecidable by proving a slightly stronger version using only a regular polygon as the basic shape of the tiles. The problem was raised by a paper of Raphael Robinson in 1971, in his famous simplified proof that the general tiling problem is undecidable for the Euclidean plane, initially proved by Robert Berger in 1966. The present construction simplifies that of the recent arXiv paper. It again strongly reduces the number of prototiles.

1 Introduction

Whether it is possible to tile the plane with copies of a fixed set of tiles was a question raised by Hao WANG, [26] in the late 50's of the previous century. WANG solved the *origin-constrained* problem, which consists in fixing an initial tile in the above finite set of tiles. Indeed, fixing one tile is enough to entail the undecidability of the problem. Also called the **general tiling problem** further in this paper, the general case, free of any condition, in particular with no fixed initial tile, was proved undecidable by Robert BERGER in 1966, [1]. Both WANG's and BERGER's proofs deal with the problem in the Euclidean plane. In 1971, Raphael ROBINSON found an alternative, simpler proof of the undecidability of the general problem in the Euclidean plane, see [23]. In that 1971 paper, Robinson raised the question of the general problem for the hyperbolic plane. Seven years later, in 1978, he proved that in the hyperbolic plane, the origin-constrained problem is undecidable, see [24]. Since then, the problem had remained open.

In 2007, I proved the undecidability of the tiling problem in the hyperbolic plane, published in 2008, see [18]. In a recent arXiv paper [20], I presented a new proof of what was established in [18]. I follow the same general idea but the tiling itself is changed. It is that of [20] but several details of the presentation are changed in the present version whose result is a new significant reduction of the number of prototiles.

In order the paper to be self-contained, I repeat the frame of the paper as well as the strategy used to address the tiling problem.

In the present introduction, we remind the reader the general strategy to attack the tiling problem, as already established in the famous proofs dealing with the Euclidean case. We assume that the reader is familiar with the tiling $\{7, 3\}$ of the hyperbolic plane. That tiling is the frame which our solution of the problem lies in. The reader familiar with hyperbolic geometry can skip that part of the paper. We also refer the reader to [16] and to [10] for a more detailed introduction and for other bibliographical references. Also, in order that the paper can be self-contained, we sketch the notion of a space-time diagram of a Turing machine.

With respect to paper [20], I append a new section devoted to the construction of an aperiodic tiling. Hao Wang mentioned in [26] that if any tiling of the hyperbolic plane were necessarily periodic then, the tiling problem would be decidable. Accordingly, the unsolvability of the problem entails the existence of an aperiodic tiling of the hyperbolic plane. Section 2 deals with that point.

In Section 3, I reuse the construction of Section 2 to establish the properties of the particular tiling which we consider within the tiling $\{7, 3\}$ and which are later used for the proof of Theorem 1.

In Section 3, we proceed to the proof itself, leaning on the definition of the needed tiles. In Subsection 3.5 we proceed to the counting of the needed prototiles. That allows us to prove:

Theorem 1 *The domino problem of the hyperbolic plane is undecidable.*

Reproducing the similar section of [20] for self-containedness, Section 4 gives several corollaries of Theorem 1. We conclude about the difference between the present paper, paper [20] and paper [18].

From Theorem 1, we immediately conclude that the general tiling problem is undecidable in the hyperbolic plane.

2 An aperiodic tiling of the hyperbolic plane

Subsection 2.1 briefly mentions the frame of our constructions. Then, in Subsection 2.4, we proceed to the construction of an aperiodic tiling of the hyperbolic plane.

2.1 The tiling $\{7, 3\}$

We assume the reader to be familiar with hyperbolic geometry. We can refer him/her to [16] for an introduction.

Regular tessellations are a particular case of tilings. They are generated from a regular polygon by reflection in its sides and, recursively, of the images in their sides. In the Euclidean case, there are, up to isomorphism and up to similarities, three tessellations, respectively based on the square, the equilateral triangle and on the regular hexagon. Later on we say **tessellation**, for short.

In the hyperbolic plane, there are infinitely many tessellations. They are based on the regular polygons with p sides and with $\frac{2\pi}{q}$ as vertex angle and they are denoted by $\{p, q\}$. This is a consequence of a famous theorem by Poincaré which characterises the triangles starting from which a tiling can be generated by the recursive reflection process which we already mentioned. Any triangle tiles the hyperbolic plane if its vertex angles are of the form $\frac{\pi}{p}$, $\frac{\pi}{q}$ and

$\frac{\pi}{r}$ with the condition that $\frac{1}{p} + \frac{1}{q} + \frac{1}{r} < 1$.

Among these tilings, we choose the tiling $\{7, 3\}$ which we called the **ternary heptagrid** in [2]. It is below illustrated by Figure 1. From now on we call it the **heptagrid**.

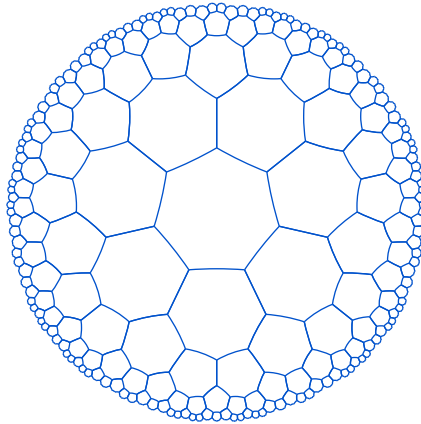


Figure 1 The heptagrid in the Poincaré's disc model.

In [2, 16], many properties of the heptagrid are described. An important tool to establish them is the splitting method, prefigured in [9] and for which we refer to [16]. Here, we just suggest the use of this method which allows us to exhibit a tree, spanning the tiling: the **Fibonacci tree**. Below, the left-hand side of Figure 2 illustrates the splitting of \mathbb{H}^2 into a central tile T and seven sectors dispatched around T . Each sector is spanned by a Fibonacci tree. The right-hand side of Figure 2 illustrates how the sector can be split into sub-regions. Now, we notice that two of these regions are copies of the same sector and that

the third region S can be split into a tile and then a copy of a sector and a copy of S . Such a process gives rise to a tree whose nodes are in bijection with the tiles of the sector. The tree structure will be used in the sequel and other illustrations will allow the reader to better understand the process.

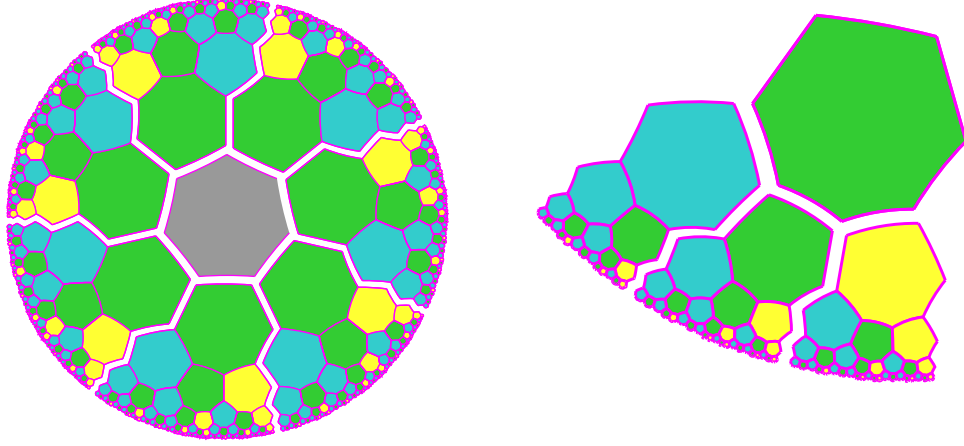


Figure 2 Left-hand side: the standard Fibonacci trees which span the heptagrid. Right-hand side: the splitting of a sector, spanned by a Fibonacci tree.

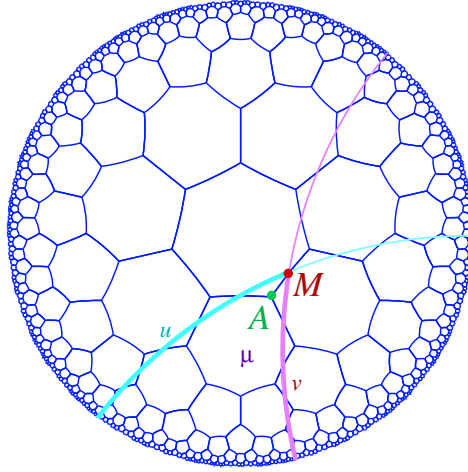


Figure 3 The mid-point lines delimiting a sector of the heptagrid. The rays u and v are supported by mid-point lines.

Another important tool to study the tiling $\{7, 3\}$ is given by the **mid-point** lines, which are illustrated by Figure 3. The lines have that name as far as they join the mid-points of contiguous edges of tiles. Let s_0 be a side of a tile. Let

M be the mid-point of s_0 and let A be one of the vertices defined by s_0 . Two sides s_1 and s_2 of tiles of the heptagrid also share A . They define a tile μ . Let u , v be the rays issued from A which crosses the mid-point of s_1 , s_2 respectively, see Figure 3. There, we can see how such rays us allow to delimit a sector, a property which is proved in [2, 16]. Later on, such a sector will be called a **sector of the heptagrid**. We say that μ is its **root** or that the sector is **rooted at μ** .

2.2 Generating the heptagrid with tiles

Now, we show that the tiling which we have described in general terms in the previous section can effectively be generated from a small finite set of tiles which we call the **prototiles**: we simply need 4 of them. The basic colours we consider are **green**, **yellow**, **blue** and **orange**: we denote them by **G**, **Y**, **B** and **O** respectively.

2.2.1 Trees of the heptagrid

Using the tiles defined previously, we define a tiling by applying the rules (R_0) also illustrated by Figure 4. The tiles we use are copies of the prototiles.

$$\mathbf{G} \rightarrow \mathbf{YBG}, \quad \mathbf{B} \rightarrow \mathbf{BO}, \quad \mathbf{Y} \rightarrow \mathbf{YBG}, \quad \mathbf{O} \rightarrow \mathbf{YBO} \quad (R_0)$$

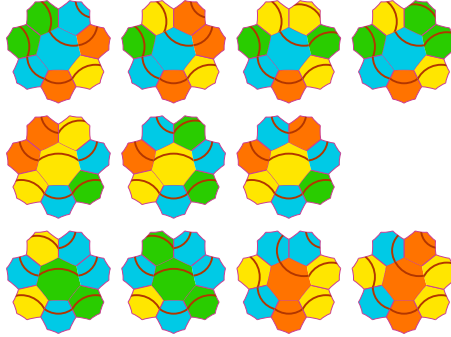


Figure 4 The prototiles generating the tiling: all cases for the neighbourhood of a tile are considered, whatever the tile: **B**, **Y**, **O** or **G**. The neighbourhoods around a tile of the same colour correspond to the different occurrences of that colour in the right-hand side part of the rules (R_0) .

Infinitely many tilings of the heptagrid can be constructed by applying the rules (R_0) with the help of Figure 4. That figure illustrates all possible neighbourhoods of tiles which are copies of the proto-tiles **G**, **Y**, **O** and **B**. We later on say that such a symbol constitutes the **status** of the tile. The first line of the figure deals with the four possible neighbourhoods for a **B**-tile: the central tile is a **B**-tile and the father is, successively, a **B**-, an **O**-, a **Y**- and a **G**-tile. As far as **Y** occurs three times in the right side of the rules of (R) , the second line of Figure 4 illustrates the possible neighbourhoods for a **Y**-tile. Next, both **G**

and **O** appear twice only in the right-hand side part of a rule of (R_0) . It is the reason why in the third line of the figure, the first two neighbourhoods concern a **G**-tile while the next two ones deal with an **O**-tile.

In order to get some order in the tiling, we introduce a numbering of the sides of each tile of the heptagrid. Assume that the side which is given number 1 is fixed. We then number the other sides increasingly while counterclockwise turning around the tile. In a tile, side 1 is the side shared with its father. As far as the central tile has no father, its side 1 is arbitrarily fixed. The neighbours are numbered after the side it shares with the tile we consider. A side receives different numbers in the tiles which share it. Table (N) indicates the correspondence between those numbers depending on the status of a tile τ and a neighbour ν . The index **g**, **y**, **b** or **o** refers to the status of ν . When the number in ν is 1 it means that ν is a son of τ .

	1	2	3	4	5	6	7	
G -tile	6 y ,7 g	7 b	1 y	1 b	1 g	2 b	3 b	(N)
Y -tile	4 y ,3 g , o	6 o , b	7 o	1 y	1 b	1 g	2 b	
B -tile	5 y ,4 g , b , o	7 y ,6 g	7 g	1 b	1 o	2 y	2 g , o	
O -tile	5 b , o	7 b	1 y	1 b	1 o	2 y	3 y	

Let us start with a few definitions needed to explain the properties which the construction needs for proving the result of the present section.

Let τ_0 and τ_1 be two tiles of the heptagrid. A **path** between τ_0 and τ_1 is a finite sequence $\{\mu_i\}_{i \in \{0..n\}}$ such that μ_i and μ_{i+1} when $0 \leq i < n$, share a side, say in that case the tiles are **adjacent**, and such that $\mu_0 = \tau_0$ and $\mu_n = \tau_1$. In that case, we say that $n+1$ is the **length** of the path and we also say that the path **joins** τ_0 to τ_1 . The **distance** between two tiles τ_0 and τ_1 is the smallest m for which there is a path joining τ_0 to τ_1 whose length is m .

Considering a sector \mathcal{S} as above defined, rooted at a tile μ , see Figure 3. We know that the set of tiles whose centre is contained in \mathcal{S} is spanned by a tree rooted at μ . In [9, 16], it is proved that such a tree is spanned by the rules of (R_0) . We call such a tree a **tree of the heptagrid** when its root is not a **B**-tile. We indifferently say that A , see the figure, is the origin of the tree or of the sector and that A points at μ . We say that the origin of the tree points at the root of the tree. We denote that tree by $T(\mu)$. Note, that a tree of the heptagrid is a set of tiles, it is not the set of points contained in those tiles. We call left-, right-hand side **border** of $T(\mu)$ the set of tiles of the tree which are crossed by the left-, right hand side ray respectively which delimit the sector defining the tree.

In a tree of the heptagrid \mathcal{T} , the **level** m is the set of tiles of \mathcal{T} which are at the distance m from the root. By induction, it is easy to prove that the sons of a tile on the level m belong to the level $m+1$.

A tiling of the heptagrid can be defined by the following process:

Construction 1

– Time 0: fix a tile τ as a root of a tree $T(\tau_0)$ of the heptagrid; that root is the level 0 of $T(\tau_0)$ and choose its status among **Y**, **G** or **O**;

– time $m+1$, $m \in \mathbb{N}$: construct τ_{m+1} as a father of τ_m , taking as τ_{m+1} with a status which is compatible with that of τ_m ; construct the level 1 of $T(\tau_{m+1})$ and for i in $\{0..m\}$, if h_i is the level of $T(\tau_i)$ constructed at time m , construct the level h_i+1 .

It is not difficult to establish the following property:

Proposition 1 *Let T_0, T_1 be two trees of the heptagrid with $T_1 \subset T_0$. Then a level of T_1 is contained in a level of T_0 . More precisely, let ρ_1 be the root of T_1 . Let h be the level of ρ_1 in T_0 . Let τ be a tile of T_1 and let k its level in T_1 . Then, the level of τ in T_0 is $h+k$.*

Proof. Let ρ_0, ρ_1 be the roots of T_0, T_1 respectively. If ρ_1 belongs to the level 1 of T_0 , the sons of ρ_1 , which belong to the level 1 of T_1 , belong to the level 2 of T_0 . Consequently, if the property is true if ρ_1 belongs to the level k of T_0 , it is also true for the trees of the heptagrid which are rooted at a tile of the level $k+1$ of T_0 . Which proves the property. \square

Below, Figure 5 illustrate two different applications of Construction 1. The left-hand side picture represents an implementation where at time 0 the initial root is a **G**-tile and, at each time, the father of τ_{m+1} is also a **G**-tile for several consecutive values of m and then, it is a **Y**-tile. In the central and in the right-hand side pictures, we have two views of the same implementation: an infinite sequence of consecutive **G**-tiles are crossed by a line ℓ so that an infinite sequence of consecutive **B**-tiles are crossed by ℓ too.

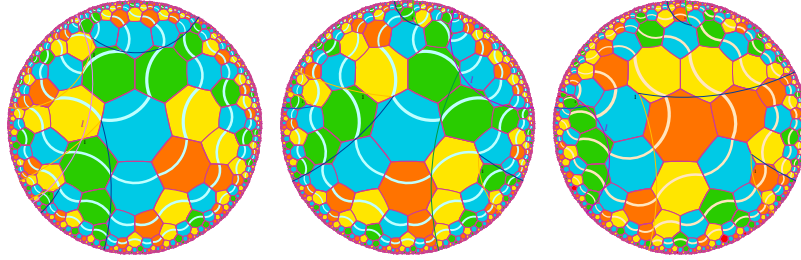


Figure 5 Two examples of an implementation of the rules (R_0) to tile the heptagrid. To left, a sequence of successive **G**- and **Y**-tiles are crossed by the same line. In the centre and to right, a sequence of **G**-tiles are crossed by the same line.

On those figures, we can notice levels for which Proposition 1 is of course true. But the figures lead us to introduce a definition. From construction 1 and from Proposition 1, we can see that a level of $T(\tau_i)$ is continued in $T(\tau_{i+1})$ and, *a fortiori*, in all $T(\tau_{i+k})$ for all positive integer k .

Proposition 2 *For any tree of the heptagrid $T(\tau)$, if μ is a non **B**-tile belonging to that tree, then $T(\mu) \subset T(\tau)$.*

Proof. It is true when μ are sons of τ or if μ is the **O**-son of the **B**-son of τ , see figure 6. Let u and v be the left- and right-hand side ray respectively issued from the origin A of $T(\tau)$.

In each of those cases, $T(\mu)$ is the image of $T(\tau)$ under an appropriate shift: a shift along u , v when μ is the **Y**-, **G**-son respectively of τ ; a shift along the left-hand side ray w defining $T(\mu)$ when μ is the **O**-son of the **B**-son of μ . Accordingly, the proposition follows for any tile ν whose status is not **B** by induction on the level of ν . \square

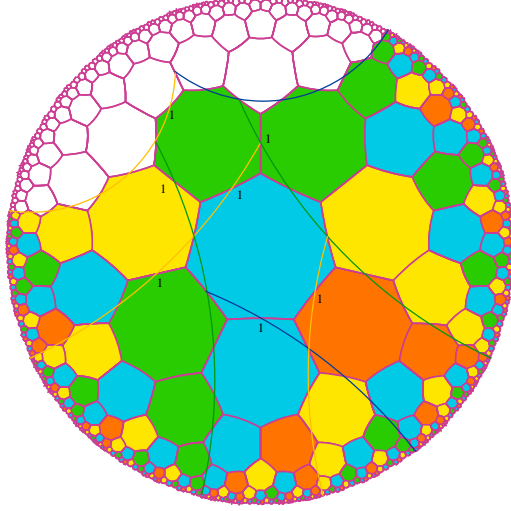


Figure 6 A tree \mathcal{T} of the heptagrid with two sub-trees of \mathcal{T} . One of them is generated by the **G**-son of the **Y**-son of the root of \mathcal{T} , the other is generated by the **G**-son of the root of \mathcal{T} . Side 1 in each tile is defined according to Table (N).

We remind the reader that in $T(\tau)$, whatever the status of τ which is assumed to be not **B**, the number of tiles belonging to the level m of that tree is f_{2m+1} , where $\{f_n\}_{n \in \mathbb{N}}$ is the Fibonacci sequence satisfying $f_0 = f_1 = 1$. If the tiles μ and ν belong to the same level of $T(\tau)$, we call **appartness** between μ and ν the number n of tiles ω_i with $i \in \{0..n\}$ such that those ω_i belong to the same level and such that $\omega_0 = \mu$, $\omega_n = \nu$ and that for i with $0 \leq i < n$, we have that ω_i and ω_{i+1} share a side. Accordingly, denoting the appartness between μ and ν by $appart(\mu, \nu)$, we get that if those tiles belong to the level m , then $appart(\mu, \nu) \leq f_{2m+1}$. From Proposition 1, it is plain that the definition of the appartness of two tiles does not depend on the tree of the heptagrid to which they belong, provided that then, they belong to the same tree.

Let us closer look at the two implementations of Construction 1 illustrated by Figure 5. Fix a **G**-tile τ of the heptagrid. Fix a mid-point A of a side of another tile sharing a vertex V only with τ . From A , draw two rays issued from A , one of them u passes through the mid-point of one of the sides of τ sharing V while v passes through the mid-point of the other side of τ sharing V . The ray u and v allow us to define a sector of the heptagrid pointed by A . Applying the rule (R_0) to τ , to its sons and, recursively to the sons of its sons, we define a tree of the heptagrid. Let v be the ray issued from A which also crosses

the **G**-son of τ . From the rules (R_0) and from Figure 4, it is not difficult to establish that in $T(\tau)$, v crosses only **G**-tiles. We can notice that time $m+1$ of Construction 1, gives us two possibilities only to define the father of a root: indeed, such a father cannot be neither a **B**-tile nor an **O**-one, as far as **G**-tiles are never sons of either a **B**-tile or an **O**-one. Figure 7 shows us what may happen when a father φ is appended to a **Y**- or a **G**-tile which is the central tile κ in the pictures of the figure, the stress being put on the corresponding trees of the heptagrid generated in that way. In the leftmost column of the figure, two pictures illustrate what happens if φ has the same status as κ . In the central column φ has the other status with respect to κ . In the rightmost column a new father ψ is appended to φ with, again, a change in the status. Note that if ψ would have the same status as φ , the obtained tree would be the same but later appendings could change the situation. Let us call the situation illustrated by the rightmost column an **alternation**. We distinguish **YGY**- and **GYG**-alternations where the symbols are self-explaining. We also note that in an alternation, the rays defining the tree rooted at ψ are both non secant with respect to the rays defined by κ , so that $T(\kappa) \subset T(\psi)$.

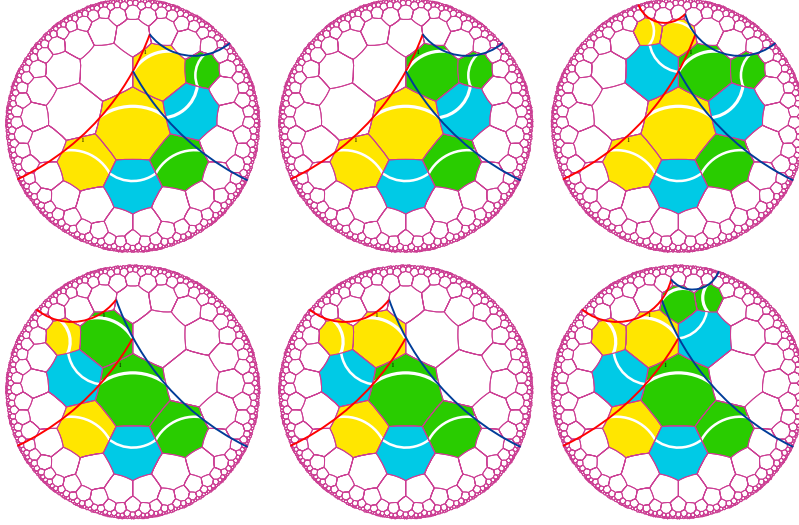


Figure 7 Appending a father to the root **Y** or **G** of a tree of the heptagrid: first line, the root is a **Y**-tile; second line: it is a **G**-tile. The rightmost column illustrates the possible alternations.

From those observations, we conclude that there are two basic situations: either, starting from a time k , the father appended at time $k+i$ has always the same status as the root at time k or, there are infinitely many times i_j , with $i_j > k$, such that the situation at times $k+i_j$, $k+i_j+1$ and $k+i_j+2$ is an alternation.

Consider the first case. There are two sub-cases: starting from a time k the appended father is always a **G**-, **Y**-tile, we call that sub-case the **G**, **Y**-ultimate

configuration respectively.

First, let us study the case of a **G**-ultimate configuration. Accordingly, we may infer that the ray issued from the origin of $T(\tau_k)$ is supported by a line ℓ which also supports the right-hand side ray delimiting $T(\tau_{k+i})$ for $i \in \mathbb{N}$. Let A_j be the origin of $T(\tau_j)$. It is not difficult to see that for $i \in \mathbb{N}$, $T(\tau_{k+i+1})$ is the image of (τ_{k+i}) under the shift along ℓ which transforms A_k into A_{k+1} . Accordingly, the left-hand side u_{i+1} ray defining $T(\tau_{k+i+1})$ and the left-hand side ray u_i defining $T(\tau_{k+i})$ are non-secant. So that the rays u_i define a partition of the half-plane π_ℓ defined by ℓ which contains $T(\tau_k)$. As a consequence, any tile μ belonging to π_ℓ falls within one of the $T(\tau_{m+i})$'s for some i . From that, we infer that there is a level λ of $T(\tau_{m+i})$ which contains μ .

What happens on the other half-plane π_r also defined by ℓ ? It is not difficult to see, as shown by the central and the left-hand side pictures of Figure 5, that ℓ also crosses a sequence of consecutive **B**-cells which lie in π_r . Let β_i be the **B**-son of the **G**-tile τ_{k+i} for $i \in \mathbb{N}$ and let ω_i be the **O**-son of β_i . Then, if u_i and v_i are the left- and right-hand side ray respectively defining $T(\omega_i)$, it can be seen that $u_{i+1} = v_i$ for all $i, i \geq k$. Indeed, the shift which transforms τ_{k+i} into τ_{k+i+1} also transforms β_i into β_{i+1} and, accordingly, it also transforms the line supporting u_i into that supporting u_{i+1} which is v_i . From that property, it easily follows that $T(\tau_{m+i+1}) \cap T(\tau_{m+i}) = \emptyset$ when $i \geq k$. Accordingly, any tile μ of π_r which is not a **B**-tile having two sides crossed by ℓ falls within $T(\tau_k)$ or within $T(\tau_{k+i})$ for some i in \mathbb{N} .

Consider the second sub-case when, starting from some k all τ_{k+i} is a **Y**-tile for all $i, i \in \mathbb{N}$. Call that case the **Y**-ultimate configuration. This time all those tiles are crossed by the line ℓ which supports the left-hand side ray defining $T(\tau_k)$. Similarly, a shift along ℓ transforms each $T(\tau_{k+i})$ into $T(\tau_{k+i+1})$. Let u_i be the left-hand side ray defining $T(\tau_{k+i})$. The same shift also transforms u_i into u_{i+1} so that those rays define a partition of the half-plane π_1 defined by ℓ which contains the τ_{k+i} 's. Accordingly, for any tile μ in π_1 , there is an integer i in \mathbb{N} such that $\mu \in T(\tau_{k+i})$.

Let π_2 be the other half-plane defined by ℓ . From Figure 4, we know that ℓ also crosses a sequence of **O**-tiles: on the level of τ_{k+i+1} , there is an **O**-tile which shares a side with that node and whose **O**-son shares a side with τ_{k+i} , being on the other side of ℓ with respect to τ_{k+i} . Let ω_{k+i} be the **O**-tile sharing a side with both τ_{k+i+1} and τ_{k+i} . From what we said, the ω_{k+i} 's belong to π_2 . The same shift as that which transforms $T(\tau_{k+i})$ into $T(\tau_{k+i+1})$ transforms $T(\omega_{k+i})$ into $T(\omega_{k+i+1})$. We can note that the $T(\tau_{k+i})$ have their right-hand side ray supported by ℓ and the left-hand side ray u_{k+i} defining that tree is such that u_{k+i+1} is the image of u_{k+i} under the shift which transforms $T(\tau_{k+i})$ into $T(\tau_{k+i+1})$. The u_{k+i} 's define a partition of π_2 so that each tile ν in π_2 belongs to some $T(\tau_{k+i})$. In fact, as far as $T(\tau_{k+i}) \subset T(\tau_{k+i+1})$, once ν is in $T(\tau_{k+i})$ it is also in all $T(\tau_{k+j})$ with $j > i$.

Consider the second case. In each τ_i defined in Construction 1, we define a segment joining the centre of that tile to the center of τ_{i+1} . The union of those segments constitute an infinite broken line which splits the complement \mathcal{C} in the hyperbolic plane of the points contained in the tiles of $T(\tau_0)$ into two parts. In

the second case, we know that there is a sequence $\{i_j\}_{j \in \mathbb{N}}$ of times, at which we have an alternation. Whether the alternation are is **GYG**, or **YGY**, we noted that the left-, right-hand side rays defined by $T(\tau_{i_j+2})$ are non-secant from the left-, right-hand side rays respectively defined by $T(\tau_{i_j})$. The consequence is that in both cases the rays defined at the alternations constitute a partition of \mathcal{C} . Accordingly, if \mathcal{T} is the set of tiles of the heptagrid, then $\mathcal{T} = \bigcup_{j \in \mathbb{N}} T(\tau_{i_j})$.

So that if μ is a tile, it belongs to $T(\tau_0)$ or to $T(\tau_{i_j})$ for some j .

That allows us to prove:

Lemma 1 *Let $\{\tau_i\}_{i \in \mathbb{Z}}$ be a sequence of tiles in a tiling constructed with the rules (R_0) , such that for all i in \mathbb{Z} $T(\tau_i) \subset T(\tau_{i+1})$. If the sequence is in an alternating configuration then, for any tile μ there is an index i such that μ falls within $T(\tau_i)$. If it is not the case:*

*If the sequence is in a **Y**-ultimate configuration. Let k be the smallest integer such that τ_i is a **Y**-tile for all $i \geq k$. Then, let ω_i be the tile sharing a side with τ_{i+1} and an other one with τ_i . Then for any tile μ there is either an index i such that μ falls within $T(\tau_i)$ or there is an index j , $j \geq k$ such that μ falls within $T(\omega_j)$.*

*If the sequence is in a **G**-ultimate configuration. Let k be the smallest integer such that τ_i is a **G**-tile for all $i \geq k$. Let β_i be the **B**-son of τ_i for $i \geq k$ and let ω_i be the **O**-son of β_i for $i \geq k$ too. Then for any tile μ which is not a β_i with $i \geq k$, there is an index i such that μ falls within $T(\tau_i)$ or there is an index j , $j \geq k$, such that μ falls within $T(\omega_j)$.*

Lemma 1 and Proposition 1 allow us to call **isocline** the bi-infinite extension of any level of a tree $T(\tau_m)$, for any value of m in \mathbb{N} . Note that Figure 4 allows us to define isoclines in a **G**-ultimate configuration by completing the levels for the exceptional **B**-tiles indicated in the Lemma and by joining the levels of the $T(\omega_i)$ with the corresponding $T(\tau_i)$.

Note that the pictures of Figure 5 also represent the tilings with their isoclines.

Let T be a tree of the heptagrid, let ρ be its root and let τ be a tile in T . Say that a path $\pi = \{\pi_i\}_{i \in \{0..n\}}$ joining ρ to τ is a **tree path** if and only if for each non negative integer i , with $i < n$, π_{i+1} is a son of π_i . It is not difficult to see that, in that case, n is the level of τ , which can easily be proved by induction on n .

A **branch** in a tree T of the heptagrid is an infinite sequence $\beta = \{\beta_i\}_{i \in \mathbb{N}}$ such that for each i in \mathbb{N} , β_{i+1} is a son of β_i . Accordingly, a tree path in T is a path from the root of T to a tile τ in T which is contained in the branch of T which passes through τ .

We can state:

Proposition 3 *Let T be a tree of the heptagrid. Let μ and ν be tiles in T . Let π_μ , π_ν be the tree path from the root ρ of T to μ , ν respectively. Then, $T(\mu) \subset T(\nu)$ if and only if $\pi_\mu \subset \pi_\nu$ and $T(\mu) \cap T(\nu) = \emptyset$ is and only if we have both $\pi_\mu \not\subset \pi_\nu$ and $\pi_\nu \not\subset \pi_\mu$.*

Proof. Assume that $\pi_\mu \subset \pi_\nu$. As far as the rules (R_0) applied to $T(\rho)$ have the same result when they are applied in $T(\nu)$ and in $T(\mu)$, we have that $T(\mu) \subset T(\nu) \subset T(\rho)$ and, clearly, from Proposition 1 we get that $\pi_\mu \subset \pi_\nu$.

Presently, consider μ and ν and let π_μ, π_ν be the tree paths from ρ to μ, ν respectively. Consider $\pi_\mu \cap \pi_\nu$. There is a tile β belonging to π_μ and π_ν such that π_β , the tree path from ρ to β satisfies $\pi_\beta = \pi_\mu \cap \pi_\nu$. Clearly, π_β is the greatest common path of $\pi_\mu \cap \pi_\nu$. Consider the case when $\beta = \nu$. It means that $\pi_\mu \subset \pi_\nu$. From what we already proved, we have that $T(\mu) \subset T(\nu)$.

Consider the case when $\pi_\mu \not\subset \pi_\nu$. In that case, the length of π_β is shorter from both that of π_μ and that of π_ν . It means that one son of π_β , say β_μ , belongs to π_μ and the other, say β_ν , belongs to π_ν and β_μ, β_ν does not belong to π_ν, π_μ respectively by definition of β . Now, μ and ν are non **B**-tiles.

If β is a non **B**-tile. We have three cases as far as μ and ν can be exchanged if needed:

- (i) β_μ is the **Y**-son and β_ν is the **G**- or **O**-son;
- (ii) β_μ is the **Y**-son and β_ν is the **B**-son;
- (iii) β_μ is the **B**-son and β_ν is the **G**- or **O**-son.

In the case (i), Figure 6 shows us that the right-hand side ray u of $T(\beta_\mu)$ and the left-hand side ray v of $T(\beta_\nu)$ have a common perpendicular which is the line containing the side of the **B**-son of β share with β . So that $T(\beta_\mu) \cap T(\beta_\nu) = \emptyset$.

In the case (ii), as far as ν is a non **B**-tile, there is a tile γ in π_ν which is a descendent of β which is the first non **B**-tile on π_ν in between β_ν and ν . It may happen that $\gamma = \nu$. In that case, all tiles on π_ν after β and until γ are **B**-tiles. As can be seen from Figure 6, those **B**-tiles are crossed by u . We have that γ is an **O**-tile and if w is the left-hand side ray of $T(\gamma)$, u and w have a common perpendicular as can be seen on Figure 6 for the **O**-son of the **B**-son of the tree which is there represented. Accordingly, $T(\beta_\mu) \cap T(\gamma) = \emptyset$. As far as $T(\nu) \subset T(\gamma)$ we again get that $T(\mu) \cap T(\nu) = \emptyset$.

In the case (iii), we can argue in a similar way. This time, let y be the left-hand side ray of $T(\beta_\nu)$. If γ is the **O**-son of β_μ , Figure 6 shows us that $T(\gamma) \cap T(\beta_\nu) = \emptyset$ as far as y is the right-hand side ray of $T(\gamma)$. Now, if π_μ does not pass through γ it passes outside the left-hand side ray z of $T(\gamma)$. Accordingly, $T(\mu) \cap T(\beta_\nu) = \emptyset$, so that, all the more, $T(\mu) \cap T(\nu) = \emptyset$.

Assume that $T(\mu) \cap T(\nu) = \emptyset$. Clearly, $\pi_\mu \not\subset \pi_\nu$ and also $\pi_\nu \not\subset \pi_\mu$. So that we have the situation depicted with $\pi_\beta = \pi_\mu \cap \pi_\nu$ and both $\pi_\beta \neq \pi_\mu$ with $\pi_\beta \neq \pi_\nu$. Consequently, if both $\pi_\nu \not\subset \pi_\mu$ and $\pi_\mu \not\subset \pi_\nu$ do not hold then necessarily $\pi_\nu \subset \pi_\mu$ or $\pi_\mu \subset \pi_\nu$ so that $T(\mu) \subset T(\nu)$ or $T(\nu) \subset T(\mu)$ holds. \square

We have an important property:

Lemma 2 *Two distinct trees of the heptagrid are either disjoint or one of them contains the other.*

The lemma is an immediate corollary of Proposition 3. Moreover, from the proof of that proposition, we clearly get the following result:

Proposition 4 *Let $T(\tau)$ be a tree of the heptagrid. Let $T(\mu)$ be another tree of the heptagrid with μ within $T(\tau)$. Let π_μ be a tree path from the root of $T(\tau)$*

to μ . Then π_μ contains at least one tile ν which is not a **B**-tile. Moreover, for any non **B**-tile ω in π_μ , we have $T(\omega) \subset T(\tau)$.

Note that in Figure 4, the curves representing the isoclines are constituted by two kinds of segments defined as follows. Those segments join the mid-points of two different sides of a tile: one kind, denoted by **w**, is defined by joining two sides which are separated by one side, namely joining side 2 and side 7; the other kind, denoted by **b**, is defined by joining two sides which are separated by two contiguous sides, namely joining side 2 and side 6 or joining side 3 and side 7. Call these marks on a tile its **level mark**. The distribution of the level marks obeys the following rules:

$$\mathbf{w} \rightarrow \mathbf{bww} \quad \mathbf{b} \rightarrow \mathbf{bw}, \quad (S)$$

Lemma 3 *It is not difficult to tile the heptagrid with the prototiles **Y**, **G**, **B** and **O** by applying the rules (R_0) so that the rules of (S) also apply if we put **w** marks on **B**-, and **O**-tiles only and **b** marks on **Y**- and **G**-tiles only.*

Proof. Inside a tree of the heptagrid, the result follows by induction on the levels. If we consider two trees of the heptagrid where one of them contains the other, the result follows from Proposition 1 which tells us that the levels of a sub-tree in a tree of the heptagrid are contained in levels of the tree. From Lemma 1, it is possible to construct a sequence of trees of the heptagrid $\{T(\tau_i)\}_{i \in \mathbb{N}}$ such that $\bigcup_{i \in \mathbb{N}} T(\tau_i)$ covers the whole hyperbolic plane, so that the lemma follows. \square

Note that in **w**-tiles, sides 2 and 7 are joined by the mark while in **Y**-tiles it is the case for sides 3 and 7 while in **G**-tiles it is the case for sides 2 and 6.

Construction 1 allow us to tile the whole hyperbolic plane in infinitely many ways. The number of such tilings is uncountable as far as at each time we have a choice between two possibilities and that the number of steps is infinite.

It can be argued that any construction of a tiling which, by definition, starts with any tile, is in some sense described by Construction 1. Indeed, whatever the starting tile, we find at some point a **G**-tile as far as in a tiling, there is a **G**-tile at a distance at most 3 of any tile μ . That distance can be observed for a **B**-tile: its **O**-son has a **Y**-son which to its turn has a **G**-son.

2.2.2 The trees of the tiling

From now on, we introduce two new colours for the tiles, mauve and red which we denote by **M** and **R** respectively. We decide that **M**-tiles duplicate the **B**-tiles when they are sons of a **G**-tile and only in that case and that an **R**-tile duplicates the **O**-son of an **M**-tile, so that the rules (R_0) are replaced by the following ones:

$$\begin{array}{llll} \mathbf{G} \rightarrow \mathbf{YMG}, & \mathbf{B} \rightarrow \mathbf{BO}, & \mathbf{Y} \rightarrow \mathbf{YBG}, & \mathbf{O} \rightarrow \mathbf{YBO} \\ & \mathbf{R} \rightarrow \mathbf{YBO}, & \mathbf{M} \rightarrow \mathbf{BR}, & \end{array} \quad (R_1)$$

As previously, the status of a tile is, by definition, its colour.

Figure 9 illustrates the application of the rules (R_1) by giving what they induce for the neighbours of a tile given its status and the status of its father. Alike what is done in Figure 4, we also define levels by using the rules (S) . As far as a **B**-tile or an **O** is **w**, **M**- and **R**-tiles are also **w**. As in Figure 4, the number of central tiles associated to a same status is the number of occurrences of the status in the right-hand side parts of the rules (R_1) .

We call **tree of the tiling** any $T(\nu)$ where ν is an **R**-tile. We repeat that a tree of the tiling is a set of tiles, not the set of points contained in those tiles. We also here indicate that, as far as **M**-, **R**-tiles behave like **B**-, **O**-tiles respectively, we later refer to **B**-, **O**-tiles only unless the specificity of **M**-, **R**-tiles is required.

From Lemma 2 we can state:

Lemma 4 *Let \mathcal{T}_1 and \mathcal{T}_2 be two trees of the tiling. Either those trees are disjoint or one of them contains the other. Moreover, a ray which delimits one of those trees does not intersect any of the rays delimiting the other tree. The same also applies to the rightmost and the leftmost branches of those trees.*

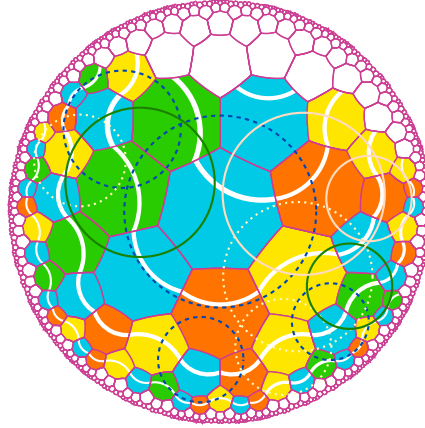


Figure 8 Figure for proving the Figures 4 and 9. The circles crosses the neighbours of the tiles which their centres. The circles have the colour of the tiles containing their centre.

Proof. Immediate from the proof of Proposition 3 when the tree are disjoint: the rays do not intersect and the property follows for the borders as far as they are inside the considered trees. We have to look at the situation when $T(\tau_1) \subset T(\tau_0)$, where $T(\tau_0)$ and $T(\tau_1)$ are two trees of the tiling. Consider the tree path π in $T(\tau_0)$ joining τ_0 to τ_1 . When going on π from τ_0 to τ_1 , let ν be the last non **B**-tile of π different of τ_1 . From Proposition 4, we know that $T(\tau_1) \subset T(\nu)$. Let u and v be the rays delimiting $T(\nu)$ and let u_1 and v_1 be those delimiting $T(\tau_1)$. We repeat here the discussion of cases (i) up to (iii) in the proof of Proposition 3. We have seen there that the same observation about the rays hold so that it extends to the borders as far as they are inside the trees

and as far as two rays cannot both cross a border. The proof of Lemma 4 is completed. \square

Figure 10 illustrates Lemma 4. Note that the figure does not mention all trees of the tiling which can be drawn within the limits of that figure.

Let us go back to the process described by Construction 1. The process leads us to introduce the following notion:

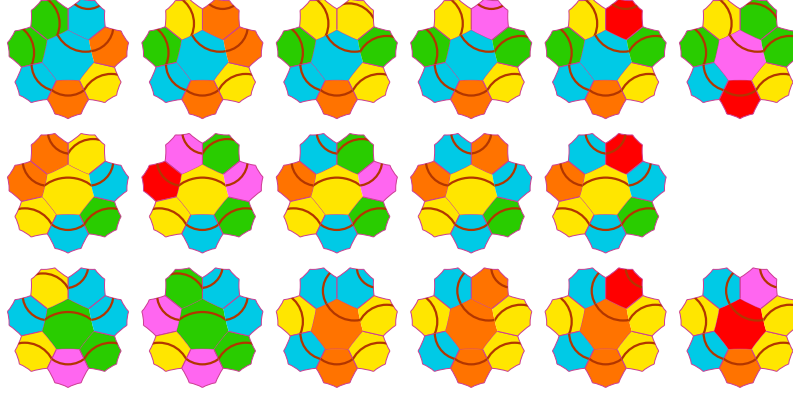


Figure 9 The prototiles generating the tiling: we describe all cases for the neighbourhood of a tile, whatever it is: **B**, **Y**, **O**, **G**, **M** or **R**. The neighbourhoods around a tile of the same colour correspond to the different occurrences of that colour in the right-hand side part of rules (R_1) .

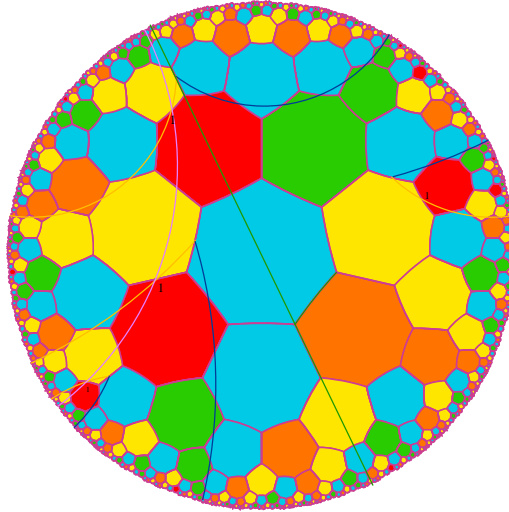


Figure 10 A tree \mathcal{T} of the tiling with three sub-trees of the tiling contained in \mathcal{T} . One of them is contained in another one while two of those trees of the tiling inside \mathcal{T} are disjoint.

Definition 1 A **thread** is a set \mathcal{F} of trees of the tiling such that:

- (i) if $A_1, A_2 \in \mathcal{F}$, then either $A_1 \subset A_2$ or $A_2 \subset A_1$;
- (ii) if $A \in \mathcal{F}$, then there is $B \in \mathcal{F}$ with $B \subset A$, the inclusion being proper.
- (iii) if $A_1, A_2 \in \mathcal{F}$ with $A_1 \subset A_2$ and if A is a tree of the tiling with $A_1 \subset A$, and $A \subset A_2$, then $A \in \mathcal{F}$.

Said in words, a thread is a set of trees of the tiling on which the inclusion defines a linear ordered, which has no smaller element and which contains all trees of the tiling which belong to a segment of the set, according to the order defined by inclusion.

Definition 2 A thread \mathcal{F} of the tiling is called an **ultra-thread** if it possesses the following additional property:

- (iv) there is no $A \in \mathcal{F}$ such that for all $B \in \mathcal{F}$, $B \subset A$.

Lemma 5 A set \mathcal{F} of trees of the tiling is an ultra-thread if and only if it possesses properties (i), (ii) and (iii) of definition 1 together with the following:

- (v) for any $A \in \mathcal{F}$ and for any tree B of the tiling, if $A \subset B$, then $B \in \mathcal{F}$.

For proving the theorem, we need a kind of converse of Proposition 4.

Proposition 5 Let A and B be two trees of the tiling with $A \subset B$. Let ρ be the root of B and let π be the tree path from ρ to the root τ of A . Let C be a tree of the tiling such that $A \subset C \subset B$. Then there is a tile ν of π such that $C = T(\nu)$.

Proof of the Lemma. Indeed, an ultra-thread satisfies (v). Assume the opposite. There are $A \in \mathcal{F}$ and B be a tree of the tiling such that $A \subset B$ and $B \notin \mathcal{F}$. Let C be another tree of \mathcal{F} . Then $B \not\subset C$, otherwise, from (iii) we get $B \in \mathcal{F}$. From Lemma 4, $C \subset B$. As far as $C \in \mathcal{F}$, we may apply to C the argument we applied to A . We get a sequence C_i of elements of \mathcal{F} such that $A \subset C_i \subset C_{i+1} \subset B$. From Proposition 5 the roots of C_i belong to the path from the root of B to that of A which is contained in a branch of B . Accordingly, as such a path is finite, the sequence of C_i is also finite. Let C_m be the biggest tree of the sequence of C_i . Repeating the argument applied to A by applying it to C_m , we get that for any C in \mathcal{F} , $C \subset C_m$ which is a contradiction with (iv). So that an ultra-thread satisfies (v).

Conversely. Assume that a thread \mathcal{F} satisfies (v). Then, it obviously satisfies (iv). \square

Proof of Proposition 5. Let, A , B and C as in the statement of the proposition. Let ρ , τ , ν be the roots of B , A , C respectively. Let π_A , π_C be the tree path from ρ to τ , ν respectively. Let ω be the tile on both π_A and π_C which is the farthest from ρ and assume that π_A and π_C go through different sons of ω . From Proposition 3 we get that $A \cap C = \emptyset$ which is impossible. So that necessarily $\omega = C$, which means that $\omega \in \pi_A$. \square

Accordingly, an ultra-thread is a maximal thread with respect to the inclusion. A thread \mathcal{F} which is not an ultra-thread is said **bounded** and there is a

tree A in \mathcal{F} such that for each B in \mathcal{F} , we get $B \subset A$. In that case, A is called the **bound** of \mathcal{F} .

Consider the following construction:

Construction 2

- time 0: fix an **R**-son ρ of a **M**-tile which is itself the son of a **G**-tile; let F_0 be $T(\rho)$;
 - time 1: at the level 3 of F_0 , and on its left-hand side border, there is another **R**-tile ρ_{-1} : let F_{-1} be $T(\rho_{-1})$; clearly, $F_{-1} \subset F_0$.
- Repeating that process by induction, we produce a sequence $\{F_i\}_{i \leq 0}$ of trees of the tiling such that F_i is contained in F_{i-1} for all negative i ; denote by ρ_i the root of F_i . If τ_{i+1} is the son of a tile τ_i , we say that $T(\tau_i)$ **completes** $T(\tau_{i+1})$.
- time $2n+1$, $n \geq 0$: complete $T(\rho_{2n})$ by $T(\rho_{2n+1})$, where ρ_{2n+1} is an **M**-tile which is the son of a **G**-tile ω_{2n+1} which we take as the **G**-son of a **Y**-tile ξ_{2n+1} ;
 - time $2n+2$: complete $T(\xi_{2n+1})$ by $T(\rho_{2n+2})$, where ρ_{2n+2} is an **R**-tile whose **Y**-son is ξ_{2n+1} ; let F_{n+1} be $T(\rho_{2n+2})$ which contains F_n .

Proposition 6 *The sequence constituted by the F_n , $n \in \mathbb{Z}$ of Construction 2 is an ultra-thread.*

Proof. By construction, $F_n \subset F_{n+1}$. Moreover, as a consequence of Lemma 4, we know that the rays delimiting F_{n+1} do not meet those delimiting F_n . The linear order follows from the construction itself. Clearly, the property (ii) is also satisfied. By construction, in between F_n and F_{n+1} there is no tree of the tiling: there are two trees of the heptagrid whose roots are not **R**-tiles. So that the sequence constitute a thread. Clearly, property (iv) is also satisfied by the construction. \square

2.3 Isoclines

We go back to the rules (S) defined in the Subsection 2.2. We proved there that it is possible to tile the plane with the rules (R_0) so that the rules (S) also apply provided that **w**-marks are put on **B**- and **O**-tiles exactly and that **b**-marks are put on **Y**- and **G**-tiles exactly. In fact, we can prove more:

Lemma 6 *Consider a tiling of the heptagrid with **Y**, **G**, **B** and **O** as prototiles obtained by applying the rules (R_0). Then, defining **w**-marks on **B**- and **O**-tiles exactly and **b**-marks on **Y**- and **G**-tiles exactly, then the **b**- and **w**-marks obey the rules of (S).*

Proof. According to the assumption, around any tile of the tiling we have the configurations of Figure 4. Now, the pictures of the figure satisfy the rules of (S) if we put **b**- and **w**-marks as stated in the assumption of the lemma. Accordingly, the tiling also obey the rules of (S) if we consider **b**- and **w**-marks only. \square

Figure 11 illustrates the property that the levels of a tree of the tiling coincide with those of its sub-trees which are also trees of the tiling. We already noticed that property for the trees of the heptagrid, see Proposition 1. That allows us to continue the levels to infinity on both sides of a tree of the tiling. We call **isoclines** the curves obtained by continuing the levels of trees in \mathcal{T} .

In the sequel, it will be important to mark the path of some isoclines on each tile of the tiling. The isoclines are unchanged if some **B**- and **O**-tiles are replaced by **M**- and **R**-ones respectively provided that rules (R_1) are applied. Figure 9 shows us that the levels are also defined in the same way.

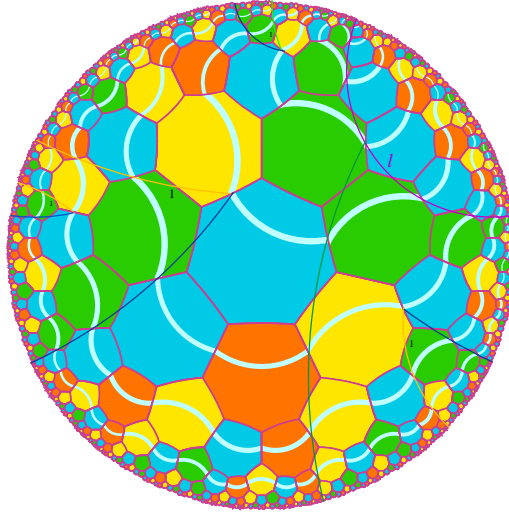


Figure 11 Illustration of the levels in the tiling. Seven of them are indicated in the figure. Four trees of the tiling are shown with the rays defining the corresponding tree of the tiling.

2.4 Constructing an aperiodic tiling

We remind the reader that in the heptagrid, a tiling is periodic if there is a shift τ such the tiling is globally invariant under the application of τ . The goal of the present subsection is to prove:

Theorem 2 *There is a tiling of the heptagrid which is not periodic. It can be constructed with 157 prototiles.*

We presently turn to the construction which will be reused to prove Theorem 1.

The idea is the following: with trees of the tiling, we define an infinite family of triangles which do not intersect and which are bigger and bigger. That property entails that the tiling cannot be periodic.

The construction is performed as follows.

We define two families of **trilaterals**, a red one and a blue one. In each family, we have **triangles** and **phantoms**, so that we have blue and red triangles and also blue and red phantoms. We call them the **interwoven** triangles as far as the blue trilaterals generate the red ones which, to their turn generate the blue trilaterals. Blue and red are the **colours** of the trilateral. Blue and red are said **opposite colours**. Triangle or phantom is the **attribute** of a trilateral. Triangle and phantom are said of **opposite attributes**.

The first steps of the construction are represented by Figure 12. Although the figure is drawn in the Euclidean plane, it can be implemented in the heptagrid.

We require that triangles of the same colour do not intersect each other. They will be implemented by following trees of the tiling as far as the borders of such a tree do not intersect those of another one. The legs of a triangle or those of a phantom will follow the borders of a tree $T(\tau)$ of the tiling. The basis of the triangle or of the phantom will follow a level of $T(\tau)$.

For properties shared by both triangles and phantoms whichever the colour, we shall speak of trilaterals. For the set of all trilaterals, we shall speak of the **interwoven triangles**.

For the construction, we consider a sequence of **R**-tiles $\{\rho_i\}_{i \in \mathbb{N}}$ such that for each i in \mathbb{N} , $T(\rho_{i+1}) \subset T(\rho_i)$, and such that ρ_{i+1} is the **R**-son of an **M**-tile which is the **M**-son of a **G**-tile which is the **Y**-son of ρ_i . We say that the pattern **YGMR** joins ρ_i to ρ_{i+1} . Now, we require that ρ_0 belongs to an isocline, chosen at random and which we call **isocline 0**. We number the isoclines with number in \mathbb{Z} . Each isocline $8n$, $n \in \mathbb{N}$ is said **green** and each isocline n with $n = 4(\text{mod}8)$ is said **orange**. Under that condition, the sequence of the ρ_i is called a **wire**. For any ρ_i we say that i is its **abscissa**. We say that ρ_{2i+1} is the **mid-point** between ρ_{2i} and ρ_{2i+2} . Note that, by construction, the mid-point lies on an orange isocline and each ρ_{2i} lies on a green isocline.

The role of the green isoclines is to construct the generation 0 of the trilaterals whose colour is blue. Each **R**-tile on a green isocline, it is called a **primary seed** triggers a trilateral, moreover, for each i in \mathbb{N} , the trilaterals raised at ρ_{2i} and $\rho_{2(i+1)}$ have the same colour and opposite attributes. The **R**-tiles on an orange isocline raise the **principal seeds** which trigger a blue or a red trilateral.

Construction 3

along each wire $\{\rho_i\}_{i \in \mathbb{N}}$ of the tiling:

step 0 defines the trilaterals of generation 0 which are blue; ρ_{2i} emit legs of a trilateral T_0 which are stopped by the isocline passing through ρ_{2i+2} ; ρ_{2i+2} emit legs of a trilateral T_1 which has the same colour as T_0 but the opposite attribute with respect to T_0 ; the ρ_{2i+1} which lies inside a triangle of generation 0 emits a red trilateral; let T_1 and T_2 be the trilaterals raised at that ρ_{2i+1} and at ρ_{2i+5} respectively for the same i ; T_1 and T_2 are both red and they have opposite attributes; accordingly, the basis of T_1 is raised at ρ_{2i+5} ; the seeds at ρ_{2i+1} also emit a mauve signal along their orange isocline from side to side;

– *step $n+1$, $n \in \mathbb{N}$: for each trilateral T of the generation n , let ρ_i be its vertex and let ρ_j emit its basis; then ρ_k is its **mid-point** where k satisfies*

$2k = i + j$; also, $j - i$ is the **height** of T ; the isocline passing through ρ_k is said the **mid-line** of T ; then for each triangle T_0 of the generation n , its mid-point emits the vertex of a trilateral T_1 and the basis of a trilateral T_2 ; T_1 and T_2 have opposite attributes and both have the opposite colour with respect to T_0 ; when the mauve signal μ emitted at step 0 is accompanied by the basis of a phantom, it is stopped by the legs of the first triangle T which it meets and the isocline of μ is the mid-line of T ; when the mauve signal is accompanied by the basis β of a triangle T , it is stopped by the first legs of the same colour as β , which completes the construction of T ; the trilaterals of the generation $n+1$ are the trilaterals whose vertex is raised at the mid-point of a triangle of the generation n .

The construction is illustrated by Figure 12.

Proposition 7 *The trilaterals of the odd generations are red, the even generations are blue. If h_n is the height of a trilateral of the generation n we have $h_n = 2^{n+1}$. The abscissa $\xi_{n,m}$ of the vertex of the m^{th} trilateral of the generation n , $m \in \mathbb{N}$, is given by $\xi_{n,m} = 2^n - 1 + m \cdot 2^{n+1}$, assuming that $\xi_{0,0} = 0$.*

Proof. As far as the trilaterals of generation 0 are blue, the trilaterals of generation 1 are red and those of generation 2 are blue so that, by induction, the trilaterals of an odd generation are red and those of an even generation are blue. By construction, the abscissas of the mid-points of the trilaterals of generation 0 are $2m + 1$, $m \in \mathbb{N}$. As far as $h_0 = 2$ trivially holds, the formula is true for generation 0. We also have that abscissas of the heads of the trilaterals of generation 0 are $2m$, $m \in \mathbb{N}$ which also satisfies the formula of the proposition. From Construction 3, as far as $\xi_{0,0} = 0$, we can see that $\xi_{1,0} = 1$. From Construction 3, we can see that $\xi_{n+1,0} = \xi_{n,0} + h_n$ as far as $h_{n+1} = 2h_n$. As far as $\xi_{0,0} = 0$, we get that $\xi_{n,0} = 2^n - 1$, from which we obtain the formula of the proposition. \square

Denote by $\mu_{n,m}$ the mid-point of the m^{th} trilateral of the generation n . From the proof of the proposition, we note that $\mu_{n,m} = (m+1) \cdot 2^{n+1} - 1 = (2m+2) \cdot 2^n - 1$ which means $\mu_{n,m}$ is also the mid-point of a trilateral of the previous generation. In fact, each second mid-point of trilaterals of the previous generations is still the mid-point of a trilateral of the generation n . The other mid-points are mid-points of triangles so that they emit vertices of trilaterals of the generation n . That proves the construction too. Note that the proof is illustrated by Figure 12. The reader is referred to the Appendix for other pictures illustrating the first five steps of the construction.

Together with Proposition 7, we have additional properties:

Lemma 7 *A trilateral T of the generation $n+1$ contains a single phantom P of the generation n and there are two triangles T_0, T_1 of the generation n such that T_0, T_1 contains the vertex, the basis of T respectively, in both cases on their mid-line. Moreover, T and P have the same mid-line. A trilateral T of the generation $n+2$ contains three trilaterals which are of the same colour of the generation n when $n \geq 1$, two of them being triangles and, in between them, a phantom P , the third one. Also, T and P have the same mid-point.*

Proof. The lemma is an easy consequence of Proposition 7.

Taking the notations of the proposition, note that

$$\xi_{n+1,m+1} = 2^{n+1} - 1 + (m+1) \cdot 2^{n+2} = \xi_{n+1,m} + 2^{n+1} = \xi_{n+1,m} + 2^n + 2^{n+1} + 2^n$$

$$\text{Moreover, } \xi_{n+1,m} = 2^{n+1} - 1 + m \cdot 2^{n+2} = 2^n - 1 + 2m \cdot 2^{n+1} + 2^{n+1} + 2^n = \xi_{n,2m} + 2^n,$$

which proves the first assertion of the lemma, as far as 2^n is half the height of T_1 . Note that the abscissa of the mid-point of T is $\xi_{n+1,m} + 2^{n+1}$ while that of T_1 is $\xi_{n,2m+1} + 2^n$. An easy computation shows as that the two abscissas are equal.

Similarly,

$$\xi_{n+2,m+1} = 2^{n+2} - 1 + (m+1) \cdot 2^{n+3} = \xi_{n+2,m} + 4 \cdot 2^{n+1} = \xi_{n+2,m} + 2^n + 3 \cdot 2^{n+1} + 2^n,$$

which proves the last part of the lemma. For what is the mid-points, the proof follows from the latter computation and from two applications of the first part of the lemma.

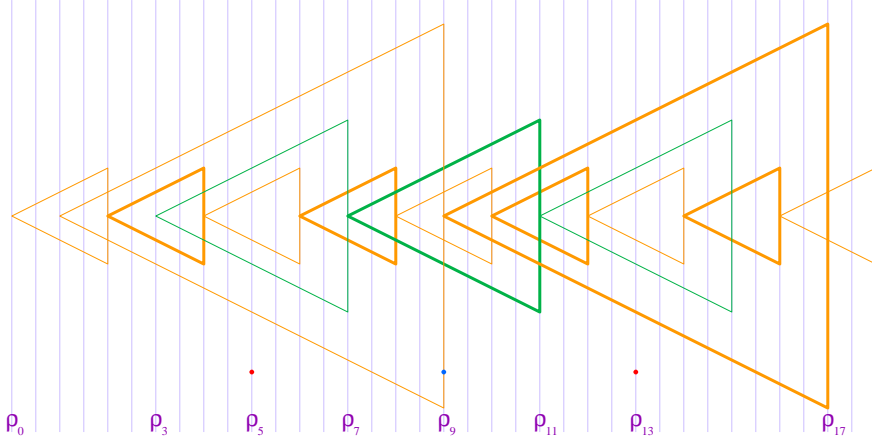


Figure 12 Illustrating the construction of the interwoven triangles. We can see how to construct a triangle of the generation $n+1$ from triangles of the generation n .

We remain with the proof that the attributes of the trilaterals we have found in the above computations are those given by the lemma. For what is the connection between a trilateral of the generation $n+1$ and the trilaterals mentioned in the lemma, we know from construction 3 that T_0 and T_1 are triangles. Consequently, the trilateral contained in T is a phantom as far as the vertex of P belongs to the basis of T_0 and the basis of P contains the vertex of T_1 . Consider a trilateral of the generation $n+2$. From what we just proved, it contains a phantom P_0 of generation $n+1$. Applying the lemma to P_0 , we get that P_0 contains a phantom P of the generation n and two triangles T_0 and T_1 such that the basis of T_0 contains the vertex of P and the vertex of T_1 belongs to the basis of P . Now, the above computations show us that T_0 and T_1 are contained

in T . That completes the proof of the lemma. \square

Proposition 8 *The legs of a trilateral do not intersect the legs of another one, whichever its colour, whichever its attribute. Moreover, two triangles of the same colour are either disjoint or one of them is embedded in the other one.*

Proof. Immediate corollary of Lemma 4 and of Proposition 7.

The colour, the attribute and the generation of a trilateral constitute its **characteristics**.

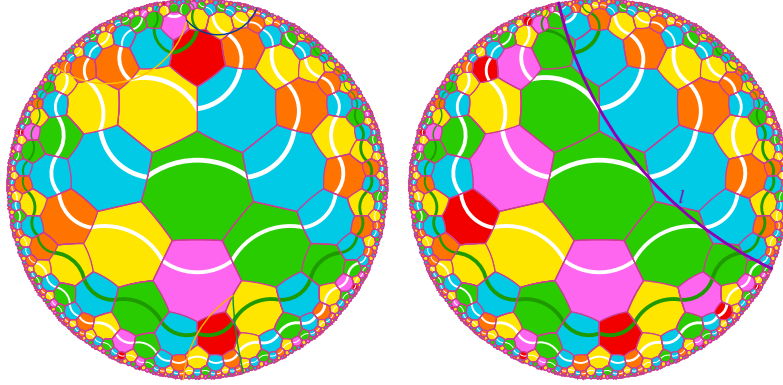


Figure 13 Representation of seeds and isoclines in two tilings of the heptagrid. To left, two trees of the tiling are illustrated, both rooted at an **R**-tile. They belong to an ultra-thread. To right, the tiling has no ultra-threads, threads only.

The trilaterals we defined in Section 2 can be embedded in the tiling of the hyperbolic plane illustrated by Figure 13. In the figure, we can see that the periodic numbering of the isoclines from 0 up to 4 is implemented with the help of three colours used to materialise the isoclines: blue, green and orange.

Proposition 9 *In each triangle T of the generation n , $n \geq 1$, its mid-line μ crosses n phantoms P_m of the generation m with $0 \leq m < n$. Moreover, μ is also a mid-line for each P_m , where $0 \leq m < n$.*

Proof. Apply Lemma 7: T contains a phantom P_{n-1} of the generation $n-1$. If $n > 1$, the lemma also applies to P_{n-1} giving rise to a phantom P_{n-2} of the generation $n-2$. By induction, we prove the proposition which is clearly true for generation 1 which follows from the previous argument. The statement about μ also follows by induction from the computation performed in the proof of Proposition 7. \square

2.5 Application to isoclines and to threads

Going back to isoclines, we already noticed that they allow to define levels in the whole hyperbolic plane. As shown by Figures 4 and 9, isoclines do not intersect

and above an isocline there is always an isocline, so that isoclines constitute a partition of the tiling. We need some additional information to Construction 2. In that construction, we defined a **wire**, denoted by \mathcal{Q} , as the sequence of tiles joining all ρ_i , $i \in \mathbb{N}$, in the tree. The sequence of $T(\rho_i)$, $i \in \mathbb{N}$ defines a thread. Remember that from ρ_i to ρ_{i+1} , both included, we have the statuses **R**, **Y**, **G**, **M** and **R** for the elements of \mathcal{Q} . Those five tiles belong to five consecutive isoclines. Note that the number of tiles of $T(\rho_0)$ which are at distance n from ρ_0 is f_{2n+1} .

Lemma 8 *Let I_n be the elements of $T(\rho_0)$ belonging to the isocline n where $n \in \mathbb{N}$. Let u_n, v_n be the leftmost, rightmost element of I_n respectively. Let y_n be the element of \mathcal{Q} belonging to the isocline n . Then*

$$\begin{aligned} \text{appart}(u_n, y_n) &\geq f_{2n-3}, \text{ appart}(y_n, v_n) \geq f_{2n-1}, \\ \text{appart}(u_n, y_n), \text{ appart}(y_n, v_n) &\leq f_{2n+1} \end{aligned} \tag{A}$$

Proof. It is plain, from Figure 9, that if ρ_i , $i \in \{1, 2, 3\}$, the status of ρ_i , i from 1 to 3, are **Y**, **B** and **O** respectively. From Lemma 2, we have $T(\rho_1) \cap T(\rho_3) = \emptyset$ and $\mathcal{Q} \setminus \{\rho_0\} \subset T(\rho_1)$. Now, consider η_j , $j \in \{1, 2, 3\}$ the sons of ρ_1 . As far as the statuses of those sons are, in the order of j , **Y**, **B** and **G** respectively, Lemma 2 tells us that $T(\eta_1) \cap T(\eta_3) = \emptyset$. Moreover, it is plain that $\mathcal{Q} \setminus \{\rho_0, \rho_1\} \subset T(\eta_3)$ and we know that $T(\eta_3) \subset T(\rho_1)$. Accordingly, we may conclude that $\mathcal{Q} \setminus \{\rho_0, \rho_1\} \cap T(\eta_1) = \emptyset$. In $T(\eta_1)$ the level of the isocline n is $n-2$ and in $T(\rho_3)$, the same isocline contains the level $n-1$ of that tree. From that, we get the estimates of (A). \square

Let us remember that Construction 2 defines an ultra-thread $\mathcal{F}_{i \in \mathbb{Z}}$, where each \mathcal{F} is $T(\rho_i)$ where the tiles joining ρ_i to ρ_{i+1} have the statuses **R**, **Y**, **G**, **M** and **R** in that order. As far as i runs over \mathbb{Z} we may, in that case, define \mathcal{Q} as a sequence of tiles indexed in \mathbb{Z} with the property that \mathcal{Q}_{4i} is exactly ρ_i . We again call that new sequence the quasi-axis of that ultra-thread. Then, it is possible to prove:

Lemma 9 *Let $\{T(\rho_i)\}_{i \in \mathbb{Z}}$ be the sequence of trees of the tiling defined by Construction 2. Then, for each tile τ of the heptagrid, there is $i \in \mathbb{Z}$ such that $\tau \in T(\rho_i)$. Accordingly, for any tile τ of the heptagrid which is not a **B**-tile, there is $i \in \mathbb{Z}$ such that $T(\tau) \subset T(\rho_i)$.*

Proof. There is an index n such that τ belongs to the isocline n . Let y_n be the tile of \mathcal{Q} belonging to the isocline n too. Let ρ_i be the closest ρ_j such that $y_n \in T(\rho_j)$ as far as, clearly, \mathcal{Q}_m belong to $T(\rho_j)$ for any j and any m starting from some value. Now, we can find $j < i$, $j \in \mathbb{Z}$, such that (A) should be satisfied with u_j and v_j being the leftmost and rightmost tiles respectively of the trace of $T(\rho_j)$ on the isocline n . Taking τ a tile of status different from **B** and from **M**, as we can find $j \in \mathbb{Z}$ such that $\tau \in T(\rho_j)$, from Proposition 4 we conclude that $T(\tau) \subset T(\rho_j)$. \square

As a corollary of Lemma 9, we can deduce the following property of the ultra-thread obtained from Construction 2:

Lemma 10 *Let \mathcal{F} be the ultra-thread given by Construction 2 and let \mathcal{G} be another ultra-thread. Then, for each tree of the tiling G in \mathcal{G} , there is a tree of the tiling F belonging to \mathcal{F} such that $G \subset F$.*

Proof. Immediate.

Proposition 10 *Let $\mathcal{F} = \bigcup_{n \in \mathbb{Z}} F_n$ be an ultra-thread and let τ_n be the root of F_n . Consider the set of levels of the tiling. For each level m in \mathbb{Z} , there is an n in \mathbb{Z} such that the level of τ_n is higher than m . Moreover, let I_m be the set of tiles on the level m belonging to F_n . Let ℓ_m, r_m be the leftmost, rightmost tile respectively in I_m . Let u in \mathbb{Z} , $u > n$. Then $I_u \subset I_m$ and $\text{appart}(\ell_m, \ell_u) \cdot \text{appart}(r_m, r_u) > 0$.*

Proof. Let h_k be the level of τ_k , k in \mathbb{Z} . Let τ_ℓ with $\ell > k$. Then, by definition of \mathcal{F} , we have $F_k = T(\tau_k) \subset T(\tau_\ell) = F_\ell$, so that $h_\ell > h_k$.

The relations concerning I_m , I_u and their respective extremal tiles comes from the fact the borders of trees of the tiling do not meet. \square

Lemma 11 *Let $\mathcal{F} = \bigcup_{n \in \mathbb{Z}} F_n$ be an ultra-thread and let τ be a tile. Then there is m in \mathbb{Z} such that $\tau \in F_m$.*

Proof. Consider a broken line \mathcal{B} which joins the centers of each τ_n , $n \in \mathbb{Z}$, where τ_n is the root of F_n . Let k be the level of τ . That level meets \mathcal{B} at some tile ν . From Proposition 10, there is an m in \mathbb{Z} such that the level of τ_m is higher than k . By construction, F_m contains ν as far as each F_n contains all the tiles crossed by \mathcal{B} , starting from its root. Let $\delta = \text{appart}(\tau, \nu)$. Let I_u, ℓ_u and r_u defined as in the proof of Proposition 10. As far as $\text{appart}(\ell_u, \ell_v) > 0$ and $\text{appart}(r_u, r_v) > 0$ if $u < v$ and as far as those appartnesses are integers, we have that $\text{appart}(\ell_u, \tau) \rightarrow \infty$ and $\text{appart}(r_u, \tau) \rightarrow \infty$ when $u \rightarrow \infty$. Accordingly, there is w in \mathbb{Z} such that $\text{appart}(\ell_w, \tau), \text{appart}(r_w, \tau) > \delta$, so that F_w contains τ . \square

Lemma 12 *There are tilings of the heptagrid with the tiles **Y**, **G**, **B**, **O**, **M** and **R** and the application of the rules (R_1) such that all its threads are bounded.*

Proof. Consider a mid-point line ℓ of the hyperbolic plane as defined in Section 2.1. Assume that ℓ crosses all the levels which can be put by a tiling of the heptagrid. It is possible to assume that ℓ crosses **G**-tiles and that the centres of those tiles lie on the same side of ℓ . Each one of those tiles generates a tree of the heptagrid whose right-hand side ray is contained in ℓ . That rules out the possibility of an ultra-thread in such a tiling. Otherwise, let $\mathcal{F} = \bigcup_{n \in \mathbb{Z}} F_n$ be an ultra-thread. Take τ as a **G**-tile crossed by ℓ . From Lemma 11, there is n in \mathbb{Z} , such that τ is contained in F_n . From Lemma 2, $T(\tau) \subset F_n$. But now, F_{n+1} contains F_n but, as its border does not meet that of F_n , that border should meet that of $T(\nu)$ where ν is a **G**-tile crossed by ℓ such that $T(\tau) \subset T(\nu)$. But in that case, we could choose ν such that its border meet that of F_{n+1} , a contradiction with Lemma 2. That proves Lemma 12. \square

Accordingly, some realisations of the tiling contain ultra-threads, some realisations of it contain none of them as illustrated by Figure 13.

2.6 The prototiles for an aperiodic tiling

From now on, we introduce a distinction of the isoclines. Each fourth isocline, starting from one of them defined at random, receives a colour: alternatively **green** and **orange**. Considering that a green isocline is higher than an orange one, that defines the directions **up** and **down** in the hyperbolic plane. The isoclines also allow us to define the directions **to left** and **to right**.

From now on, an **R**-tile will be called a **seed**. The seeds which are crossed by a green isocline are the vertices of a trilateral of the generation 0, so that they trigger the construction of that trilateral. A seed which sits on an orange isocline is the vertex of a trilateral of the generation n with $n \geq 1$. An isocline which is neither green nor orange is said to be **blue**.

In the present subsection, we implement Construction 3 as a tiling. To that purpose, we define a set of **prototiles**: the tiles of the tiling are copies of prototiles. By copy we mean an isometric image which place a tile from an isocline onto another one such that left, right up and down of the former place coincide with those directions on the new isocline. Figure 14 defines the tiles required for the implementation of the isoclines.

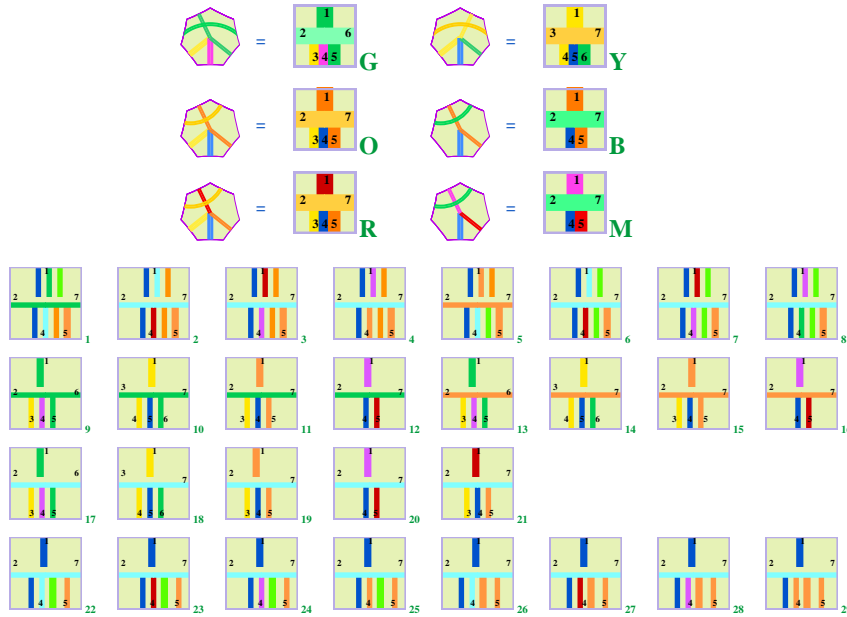


Figure 14 Implementation of the rules (R_1) and of the isoclines by 29 prototiles. Note the convention for representing heptagonal tiles by squares.

To force the succession of green and orange isoclines, we use the **B**-tiles as far as they occur in most rules in (R_1) . Tiles 1 up to 8 of the figure illustrate how we define that succession. Tiles 9-12, 13-16 and 17-21 illustrate the other

tiles than **B**-ones when they receive a green isocline, an orange one and a blue one respectively. Note that **R**-tiles are mentioned with blue isoclines only as far as they are seeds when sitting on a green or an orange isocline. The last row illustrates the tiles needed to start marking the **B**-tiles: it is the case for the son of a **Y**-, an **O** or an **R**-tile. Depending on the isocline of the father of such a **B**-tile and the surrounding isoclines, we have the appropriate tile to be synchronised with **B**-tiles on the same isocline as far as green and orange isoclines split the hyperbolic plane into two halves.

Consider a tree of the tiling $\mathcal{T} = T(\tau)$, rooted at τ . Define $\{\beta_i\}_{i \in \mathbb{N}}$ to be the branch of \mathcal{T} as follows. If τ is a **G**-tile, then $\beta_0 = \tau$. Otherwise, β_0 is the **B**-son of the **M**-son of τ . Then, for any non negative integer n , β_{n+1} is the **B**-son of β_n . Call that branch the β -branch from τ . We say that the branch consists of τ and of its recursive **B**-off-springs. The interest of that definition is that the β -branch of \mathcal{T} does not intersect any tree of the tiling contained in \mathcal{T} .

It can easily be seen from Figure 9 that the prototiles of the figure can tile $T(\tau)$. The first three rows of the figure indicate the convention we use to represent the heptagonal prototiles by square ones. The convention is based on the fact that we have mainly a top down direction and a left right one given by the isoclines. The top number indicates 1, the side to the father. At the bottom side of the square we have the numbers of the sides to the sons of the tile. On the left- and right-hand side edges, we have the number of the sides crossed by the isocline on which the tile sits.

As an example, it is not difficult to see that a **w**-tile cannot abut another **w**-tile and that, similarly, a **b**-tile cannot abut another **b**-tile. From that and similar considerations we leave to the reader, the tiles with a blue isocline can build the pictures of Figure 9 and only them. As far as besides the isocline the tiles with a green isocline of Figure 14 look like those with a blue isocline, we obtain the pictures of Figure 9 and only them with the tiles of Figure 14. We also clearly obtain that green and blue isocline do not mix and do not cross each other. The first row of Figure 14 allow us to build a β -branch in any tree of the tiling. But the first row alone generates a β -branch whose root is rejected at infinity. For a true β -branch rooted at a tree of the heptagrid, we need the tiles of the last row of Figure 14: the father of a **B**-tile is either a **Y**-, an **O**- or an **R**-tile. In each case, the father may be on a green or on a blue isocline while the **B**-tile may be on a blue or on a green one. Of course, if the **B**-tile, its father is on a green tile then its father, the **B**-tile respectively, is on a blue one.

Note that the green, orange isocline defined by a first tile 1, 5 respectively impose the position of all other green, orange isoclines by the fact that the tiles bearing a green, orange isocline can only abut on the same level tiles also bearing a green, orange isocline respectively.

In order to define the prototiles to construct the trilaterals, we need another property which can be deduced from Proposition 7 and Lemma 7:

Proposition 11 *The legs of a trilateral T of the generation $n+1$ are cut once by the basis B of the triangle T_0 of the generation n whose mid-point is the vertex V of T . That isocline β which contains B is issued from ρ_j where ρ_j is*

the mid-point between V and the mid-point of T . In between V and β , the legs of T are cut by bases of phantoms only. In between β and the basis of T , the legs of T are not cut by any trilateral of whichever generation.

Proof. From Lemma 7, we know that the vertex of T is the mid-point of a triangle T_0 of the generation n and that the basis of T is issued from the mid-point of a triangle T_1 of the generation n too. As far as the height of T_0 is the half of that of T the basis of T_0 satisfies the statement of the proposition. Some trilaterals of generation m , with $m \leq n$ whose vertices are contained in T cut the basis of T , but their basis does not cut the legs of T . For what are trilaterals of generation higher than $n+1$, either they contain T or they are disjoint from T so that in both cases, their basis do not cut the legs of T . \square

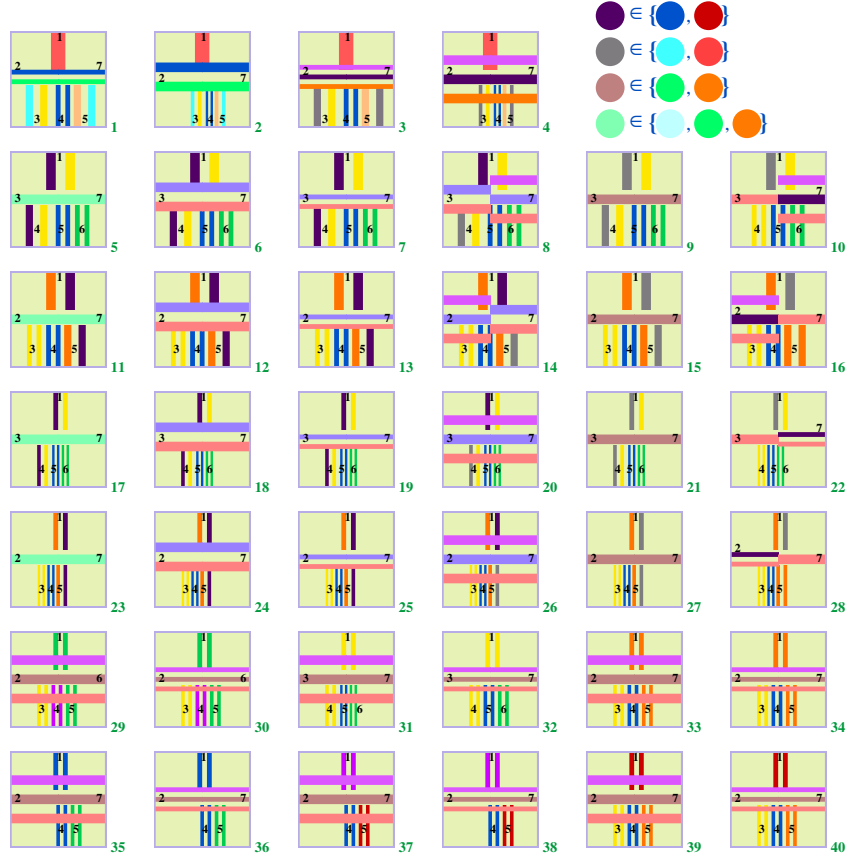


Figure 15 The 128 prototiles for constructing the trilaterals. Among those prototiles, 28 of them represent a red or a blue trilateral. Note the conventions of colours in order to restrict the number of pictures down to 40 of them.

Figure 15 gives the prototiles for constructing the trilaterals which have to be appended to those of Figure 14. Note that the prototiles 1 to 4 of Figure 15

complete the prototiles of Figure 14 for what are the seeds on a green or an orange isocline.

The first row of the second part of Figure 15 illustrates prototiles to trigger the construction of the legs of a trilateral. Note that both left- and right-hand side legs are represented. Moreover, as indicated by the figure itself, we use a few grey colours to be replaced by various hues of blue and red. It is the reason why the 128 prototiles are illustrated by only 40 ones. In fact, as indicated in the propositions and lemmas devoted to the trilaterals, the legs can be uniformly dealt with. Note the fact that for a leg, whichever its side is, we use two hues of the same colour: a dark version for the first half of the leg starting from the vertex, and a lighter version for the second half. The rightmost part of the first row in the second part of the figure illustrates three conventions we use for the hues which represent two or three colours.

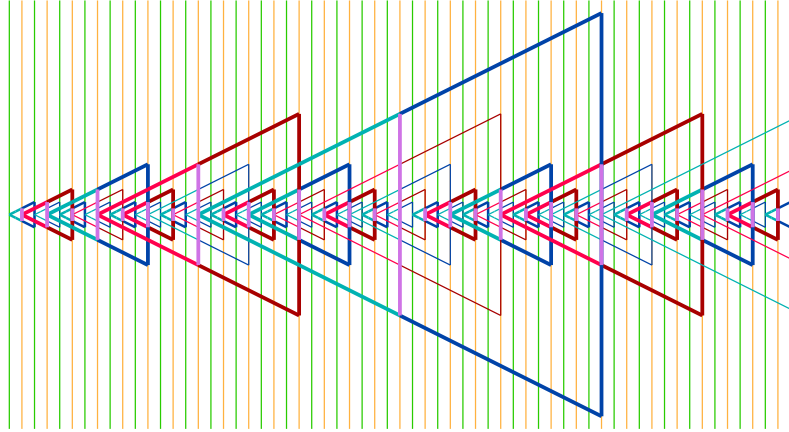


Figure 16 The construction of an aperiodic tiling.

Consider a **triangle** T whose vertex is denoted by V and its mid-point by ω . From Proposition 11, the first basis of a *triangle* T_0 cutting a leg of T cuts the path from V to the basis of T at the mid-point ν between V and ω . Such a basis met by a leg when running over it from V occurs at the fourth of the leg. From Lemma 7, the other bases cutting the leg of T in between V and ν are bases of trilaterals of lower generations. Clearly, the mauve signals running on the isoclines of those bases meet triangles of a generation lower than that of T_0 , so that when those bases cut the leg of T there is no mauve signal with them. So that the first time a leg of T meets a mauve signal, it is on the isocline passing through ω . Accordingly, the change of colour for the leg of T occurs at that moment. Later, there is no meeting of a basis of a trilateral, the basis of T being excepted. When it is the case, the basis does not contain a mauve signal at that meeting.

Accordingly, the proof of Theorem 2 is completed. The number of needed prototiles is the sum of the numbers indicated in Figures 14 and 15. \square

Figure 16 illustrates the proof of Theorem 2.

3 Completing the proof of Theorem 1

Presently, we shall see how to obtain the prototiles we need in order to prove Theorem 1. It is important to see that the theorem will be proved only when we have produced the set of prototiles.

From the previous construction, we know that we have bigger and bigger triangles, so that if we take red triangles as the frame of the simulation of a Turing machine, it is a possible solution. It is enough that the set of prototiles is adapted to a given Turing machine M in order to perform its computation in any triangle. If M does not halt, the computation is stopped when the computing signal meets the basis of the triangle and it will be the case in all triangles. If M halts, the halting will be observed in some triangle. It is easy to implement the halting state by a prototile one side of which cannot be abut by any prototile.

However, that program can be fulfilled if we can perform the computation in a red triangle. The scenario is the following. The initial configuration is displayed along the right-hand leg ℓ_r of the red triangle T . That leg consists of **O**-tiles, the vertex of T being excepted: it is the tile 15.3, an **R**-tile sitting on an orange isocline. From the **O**-tiles, we consider the path in T which goes from a tile τ of ℓ_r to a tile of the basis of T by following the **Y**-son of τ and, recursively, the **Y**-sons of those **Y**-sons. Call such a path the **Y-path from** τ and say that τ is its **source**. From Lemma 2, we know that a **Y**-path from a tile ℓ_r does not meet the legs of a triangle contained in T . The role of a **Y**-path from τ is to convey the content of the square of the tape of M which lies in τ . The **Y**-path updates that content as soon as the appropriate state is seen, so that the **Y**-path records the history of the computation on the square represented by its source. A computing signal ξ starts from the root ρ of T and it visits the **Y**-paths according to the program of M . In order to go from one **Y**-path to the next one, the ξ travels on a level of $T(\rho)$. That signal conveys the current state η of M . When ξ meets a **Y**-path conveying the current content σ of the square of the tape which is the source of that **Y**-path, ξ performs the instruction associated to η and σ in the program of M . The **Y**-path convey the new letter contained by the square at the source of the **Y**-path. It also conveys the new state of M as well as the direction δ towards the **Y**-path whose source is a neighbour of the source from which the previous **Y**-path originated. To that goal, ξ goes to the next level along the **Y**-path it met and, on that level, goes to the new **Y**-path in the direction given by δ .

As far as T may contain other red triangles in which the same computation of M is performed, those computations should not interfere with each other. We already know that the **Y**-paths generated in T do not meet those of a triangle inside T . It is also necessary that the levels on which ξ travels in T are not those on which a similar signal travels in a triangle contained in T . Accordingly, we have to deal with that point.

Call **free row** of a trilateral T , the intersection with T of an orange or a green isocline which does not meet the legs of a triangle contained in T . Note that the notion might be applied to red phantoms as well but we reserve it for red triangles. We deal with that problem in Subsection 3.1.

We also notice from Figure 15 that active seeds trigger both the construction of legs of a trilateral T and the construction of the basis of a trilateral whose status is opposite to that of T . However, as indicated by Figure 13, it may happen that the basis triggered by an active seed will not meet legs of an appropriate triangle. It is the case if the tree of the tiling raised by the active seed is the bound of a thread. That raises another problem dealt with in Subsection 3.2.

3.1 Free rows in red triangles

Before considering how to detect the free rows in a red triangle, it is important to know whether there are enough of them for the computation purpose.

Lemma 13 *In a red trilateral of the generation $2n+1$ there are $2^{n+1}+1$ free rows.*

Proof. The smallest generation for a red triangle is generation 1 and such a triangle contains two green isoclines and one green one. Accordingly, such a triangle contains 3 free rows. From Lemma 7, a red triangle T of the generation $2n+3$ contains two red triangles T_0 and T_1 of the generation $2n-1$ with, in between them, a phantom of that generation which contains φ_{2n-1} free rows. The height of T is four times that of T_0 . It is not difficult to see that the vertex of T is contained in a phantom P_0 of the generation $2n-1$ too and that the vertex of T is the mid-point of P_0 . Similarly, the basis of T is contained in the mid-line of a phantom P_1 of the generation $2n-1$ too. Accordingly,

$$\varphi_{2n+1} - 1 = 2(\varphi_{2n-1} - 1)$$

which gives us

$$\varphi_{2n+1} = 2\varphi_{2n-1} - 1 \quad (*)$$

as far as the mid-line T is counted twice if we consider $2\varphi_{2n-1}$. An easy induction from $(*)$ shows us that $\varphi_{2n+1} = 2^{n+1} + 1$. We again find that $\varphi_1 = 3$. We can check on Figure 24, see the Appendix, that $\varphi_3 = 5$. \square

Note that a red triangle of the generation $2n+1$ is crossed by $4^{2n+2} = 8^{n+1}$ isoclines. Accordingly, if the number of free rows of a red triangle of the generation $2n+1$ is very small with respect to its height, it still tends to infinity as n tends to infinity.

It is worth noticing that if we choosed the blue triangles instead of the red ones in order to simulate the computation of the Turing machine, using a similar definition for free rows with the help of blue signals instead of the red ones, we would obtain that in each blue triangle there is a single free row, the mid-line of the triangle, see [18] for the proof. The reason is that generation 0 consists of blue trilaterals in which there is a single free row while in a red triangle of generation 1 there are three free rows.

Accordingly, it is worth dealing with the detection of the free rows in red triangles. To that aim we proceed as follows. The legs of a red triangle T send a

red signal inside T along a green or an orange isocline. If the signal meets a leg of the same side and of the same colour, the signal goes on. It goes on too if it meets the legs of a blue triangle or the legs of a phantom, whichever the colour. If the signal meets a leg of an opposite side, we prevent tiles to implement such a meeting. We also give the leg the possibility to send a yellow signal inside T along a such an isocline. If the signal meets a leg of an opposite side, it is the other leg of T and the signal is established: a free row is detected. If the yellow signal meets a leg of the same side, it means that it must be replaced by a red signal as far as no tile implements the crossing of the yellow signal by a leg of a red triangle. However, the yellow signal may freely cross legs of blue triangles and of phantoms whatever their colour. Accordingly, each green or orange isocline inside T conveys a signal: a red one if on that isocline the signal meets the leg of a red triangle inside T , a yellow one if on that isocline the signal does not meet a red triangle inside T . In Subsection 3.5 we shall see how the problem is solved.

3.2 Synchronisation

We already noted the problem of possible active seeds which are the origin of a bound for some bounded thread.

Another problem arises: as far as on the same green or orange isocline there might be several seeds, it is important that the red signals raised in a triangle occurs on the same isocline as a yellow signal inside another triangle. Call **latitude** a finite set of consecutive green and orange isoclines. The **latitude of a trilateral** is the set of green and orange isoclines from the isocline of its vertex to that of its basis.

Note that the lateral red signals give rise to signals which may travel along an isocline far away from the legs of any triangle. Those signals of opposite laterality may meet in between two red triangles and outside them: in that case, a left-hand side signal coming from right meets a right-hand side signal coming from left. It is important that the latitude of a trilateral coincide with that of trilaterals of the same characteristics belonging to different threads. The red signals used for detecting the free rows are not enough for that property.

To better see what is involved, we need the following notion. Consider a trilateral T of generation $n+1$. If the vertex V of T is inside a triangle T_1 , we say that T_1 is the **father** of T . Note that a trilateral may have no father: it is the case in a wire defined by a bounded thread. If T has a father of T_1 we may define the father of T_1 if that later exists. Accordingly, for any trilateral T , we construct a sequence $\{T_k\}_{k \in [0..h]}$ such that $T_0 = T$ and for each k in $[0..h-1]$, T_{k+1} is the father of T_k and T_h has no father. Each T_k with k in $[0..h]$ is called an **ancestor** of T and T_h is called the **remotest ancestor** of T . Note that the generation of the remotest ancestor of a trilateral T depends on the wire to which T belongs.

We append two kinds of signals. We consider a special signal for blue trilaterals: the vertex of a blue trilateral as well as the ends of its basis trigger a **blue** signal, the same one whichever the laterality of the end emitting it, whichever

the attribute of the trilateral. Such a signal is important due to the fact that a thread may not cross the latitude of a given trilateral. Also, to distinguish latitudes of red trilaterals we need to mark the isoclines passing through the heads of red triangles. We call that latter mark the **silver** signal. It is raised by the vertex V of a red triangle and it travels on the orange isocline which passes through V .

The silver and the blue signals allow us to prove the following property:

Lemma 14 *Let T be a trilateral belonging to a wire \mathcal{W} . Let S be a trilateral whose characteristics are those of T , S belonging to a wire \mathcal{V} , with $\mathcal{V} \neq \mathcal{W}$. Then T and S has the same latitude if and only if T , S have an ancestor X , Y respectively, such that the vertex of X and that of Y lie on the same isocline.*

Note that the lemma mentions an ancestor within the same latitude and it says nothing of the remotest ancestors of T and S which may belong to different latitudes. As a consequence of the lemma, we can say that the latitudes of red triangles of the generation $2n+1$ are the same whatever the wire giving rise to the interwoven triangles and for any $n \in \mathbb{N}$.

Proof of Lemma 14. We prove that property by induction on n , for $n \geq 1$. Note that for any trilateral T of generation 0, its ancestors are T itself. Consider a triangle T of generation 0 in \mathcal{W} . Its vertex W sits on a green isocline ω . If ω meets a seed V belonging to \mathcal{V} , V receives the blue signal emitted by W as far as that signal cannot leave ω : that signal may be interrupted by a basis lying on ω , but that very basis restores the signal starting from its ends. Accordingly, W triggers a trilateral S of generation 0. The colour of S is the same as that of T , we remain with its attribute. What we have seen up to now shows us that the trilaterals of generation 0 lie within the same latitudes both for \mathcal{W} and for \mathcal{V} . We have to see that the attributes are the same for the same latitude. Let A be the mid-point of T . It triggers a trilateral Q of generation 1. If Q is not a triangle, its basis defines a seed B of \mathcal{W} which triggers a triangle H . It is not difficult to see that B belongs to a triangle J of generation 0 whose vertex is on the basis of the phantom whose vertex is on the basis of T . Accordingly, we may assume that Q is a red triangle. Now Q emits a silver signal which travels on its orange isocline ϖ which meets a seed C of \mathcal{V} . As far as isoclines cannot cut each other, the distance from W to A is the same as the distance from V to C . And so, C is the mid-point of S which raises a red triangle. Consequently, S is a triangle too. We proved the lemma for generation 0. The argument of the silver signal to identify the attribute of S show us that the lemma is also true for generation 1.

Assume that the lemma is true for the generation n . Consider a trilateral T of the generation $n+1$ whose vertex is in \mathcal{W} . We may assume that T is a triangle: if it were a phantom P we would consider as T the triangle triggered by the seed of \mathcal{W} lying on the basis of P . Let W be the vertex of T and let N be its mid-point. We know that on the same wire, there is a seed Q which also triggers a triangle of the same colour as T and the distance of Q from W is twice the height of T . Let ω , ϖ and φ be the isoclines passing through W , N

and Q respectively. Let V , M and P be the seeds of \mathcal{V} lying on the isoclines ω , ϖ and φ respectively. The distance from V to P is that from W to Q which means that the trilateral issued from V has the same height as T so that its generation is the same and its colour is also the same. Also, M is the mid-point of S . Clearly, if T is a red triangle, so is S as far as the silver signal emitted by W passes also through V . If T is blue, N triggers a red trilateral and, arguing like we did for generation 1, we may assume that N triggers a red triangle. Accordingly, M also triggers a red triangle as far as it receives the silver signal emitted by N . Now, a triangle is triggered at the mid-point of another triangle, so that S is a triangle too as far M is its mid-point. Consequently, we proved that for the generation $n+1$ the latitudes are the same for trilaterals with the same attributes, provided that the trilateral are both present in \mathcal{W} and in \mathcal{V} .

From that, the lemma follows. If S and T have the same latitude, their attributes are the same and their ancestors lie within the same latitudes as long as they are present in both wires. If T and S have an ancestor whose vertices are on the same isocline, clearly, those ancestors have the same latitude and, step by step, their successive sons occupy the same latitudes, so that it is the case for S and T too. \square

Later on, we refer to Lemma 14 when we say that the silver and the blue signals allow us to synchronise all wires of the tiling.

The problem raised by possible bounds of threads is dealt with as follows. The blue signal emitted by a the basis of a trilateral of a wire may meet the basis emitted on the same isocline by a blue trilateral of another wire. Such a meeting is permitted: it solves the problem of possibly missing trialterals in a bounded thread.

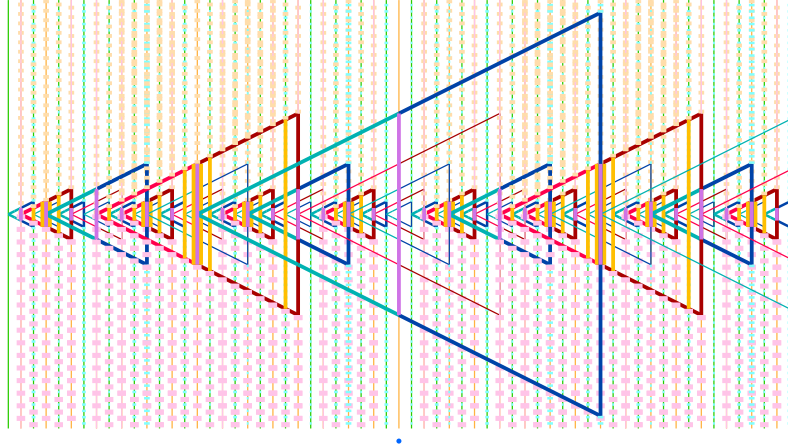


Figure 17 The free rows in the red triangles. They are in yellow in the figure. Note that the yellow signal is superposed with the mauve one on the mid-line of red triangles.

From our description of the signals emitted by the legs of a triangle in order to detect free rows inside them, we can see that such signals must cross legs

of the same laterality. It is the reason why we consider that instead, the legs of a red triangle emit a red signal of their laterality outside the triangle. As illustrated by Figure 17, we can see that a red signal emitted by a red triangle T_0 included into another red triangle T_1 also cuts the legs of T_1 . Those red signals are similar to the blue signals above defined for both trilaterals. The difference is here that they concern red triangles only and that they are not emitted by the vertex and the basis only: they are emitted on each green or orange isocline crossing the leg. We also decide that right-, left-hand side red signals coming from left, from right respectively may match with a red basis coming from right, from left respectively.

Note that appending the silver signal means just changing a bit the tiles conveying an orange isocline, but it also requires to append five tiles as far as there are tiles outside legs and bases of trilaterals which convey an orange isocline with no signal at all.

We remain with the condition meant by the *general tiling problem*. We borrow the next subsection to paper [18] with a few changes.

3.3 The general tiling problem

In the proofs of the general tiling problem in the Euclidean plane by Berger and by Robinson, there is an assumption which is implicit and which was, most probably, considered as obvious at that time.

Consider a finite set S of **prototiles**. We call **solution** of the tiling of the plane by S a partition \mathcal{P} such that the closure of any element of \mathcal{P} is a copy of an element of S . We notice that the definition contains the traditional condition on matching signs in the case when the elements of S possess signs. We also notice that a copy means an isometric image. In that problem, we assume that only shifts are allowed and we exclude rotations. Note that, in the Euclidean case, rotations are also ruled out. Here rotations have to be explicitly ruled out as far as the shifts leaving the tiling globally invariant also generate the rotations which leave the tiling globally invariant. In fact we accept isometries and only those such that a tile marked **w** or **b** on a given isocline is transformed into a tile marked **w** or **b** respectively on an isocline, the same one or another one.

Note that the general tiling problem can be formalized as follows:

$$\forall S \quad (\exists \mathcal{P} \text{ sol}(\mathcal{P}, S) \vee \neg(\exists \mathcal{P} \text{ sol}(\mathcal{P}, S))),$$

where $\text{sol}(\mathcal{P}, S)$ means that \mathcal{P} is a solution of S and where \vee is interpreted in a constructive way: there is an algorithm which, applied to S provides us with 'yes' if there is a solution and 'no' if there is none.

The origin-constrained problem can be formalized in a similar way by:

$$\forall (S, a) \quad (\exists \mathcal{P} \text{ sol}(\mathcal{P}, S, a) \vee \neg(\exists \mathcal{P} \text{ sol}(\mathcal{P}, S, a))),$$

where $a \in S$, with the same algorithmic interpretation of \vee and where the formula $\text{sol}(\mathcal{P}, S, a)$ means that \mathcal{P} is a solution of S which starts with a . Note that if a is a blocking tile, *i.e.* a tile which cannot abut any one in S , then we may face a situation where we cannot tile the plane because a was chosen at random while it is possible to tile the plane. A solution is to exclude a from

the choice. The other one is to allow the occurrence of contradictions because a wrong tile was chosen while the appropriate one would raise no contradiction. Of course, there must be a restriction: such a change should occur finitely many times at most for the same place.

Obviously, if we have a solution of the general tiling problem for the considered instance, we also have a solution of the origin-constrained problem, with the facility that we may choose the first tile. To prove that the general tiling problem, in the considered instance, has no solution, we have to prove that, whatever the initial tile, except the blocking one, the corresponding origin-constrained problem has no solution either.

In Berger's and Robinson's proofs the construction starts with a special tile, called the **origin**. Their proof holds for the general problem as far as they force the tiling to have a dense subset of origins. In the construction, the origins start the simulation of the space-time diagram of the computation of a Turing machine M . All origins compute the same machine M with the same initial configuration of M . The origins define infinitely many domains of computation of infinitely many sizes. If the machine does not halt, starting from an origin, it is possible to tile the plane. If the machine halts, whatever the initial tile, we nearby find an origin and, from this one, we shall eventually fall into a domain which contains the halting of the machine: at that point, it is easy to prevent the tiling to go on.

The present construction aims at the same goal.

From Proposition 7, we know that the trilaterals are bigger and bigger once their generation is triggered along a wire. Consequently, what we suggested with the **Y**-paths and the free rows answer positively the possibility to simulate any Turing machine working on a semi-infinite tape which, as well known, does not alter the generality. We remain with the way to force such computations.

3.4 The seeds

We establish that there are enough seeds for starting the computation of a Turing machine in the interwoven triangles.

We have the important property:

Lemma 15 *Let the root of a tree of the tiling T be on a green or an orange isocline. Then, there is a seed in the tiles of T on the next orange or green isocline respectively, downwards. Starting from that last isocline, there are seeds, downwards, on all the isoclines.*

We have a very important density property:

Lemma 16 *For any tile τ in a tiling, fitted with the isoclines, there is a seed on a green or an orange isocline within a ball around τ of radius 8.*

Proof. From Figure 9 we can see that if we consider a **G**-tile τ , there is a seed at a distance 2 from τ . As far as a **Y**-tile has a **G**-son, there is a seed at a distance at most 3 from a **Y**-tile. By construction, there is a seed at distance 1

from an **M**-tile. Figure 9 shows us that there is a **G**-tile at distance 1 from a **B**-tile. Accordingly, there is a seed at distance at most 3 from a **B**-tile. There is a **Y**-tile at distance 1 from an **O**-tile so that there is a seed at distance at most 4 from an **O**-tile. Accordingly, there is another seed at distance at most 4 from a seed. If the seed found in that way is on a green or an orange isocline, four isoclines further there is a seed on a green or on an orange isocline at distance at most 8. \square

From Lemma 16, we know that around any tile τ there is a seed in a disc of radius 4. We can say a bit more:

Lemma 17 *Assume that there is a seed on a green isocline. Then, there is at least a seed on the next green isocline and on each further isocline whichever its colour.*

Proof. Let τ be a seed on an isocline. From Lemma 16 it can be easily found everywhere. Say that the isocline to which τ belongs is isocline 0. The sons of τ , say τ_i , $i \in \{1..3\}$ are not seed and none of them is **M**. Accordingly there is no seed on the levels 1 and 2 of $T(\tau)$. On the level 2 the statuses of the sons of the τ_i , $i \in \{1..3\}$, are **Y**, **B**, **G** or **O**. Accordingly, there is no seed on the level 3 but as far as there is a tile **M** on that level, there is a seed on level 4. But a **G**-tile always has a **G**-son so that if the **G**-tile on level 2 raises a seed on level 4 the **G**-descendants of that tile generate a seed at each level n with $n > 4$. At least one of those isoclines is green so that we can repeat the argument. That completes the proof of the lemma. \square

From now on, a seed on a green or an orange isocline is called an **active seed**.

In each red triangle, we define a limited grid in which we simulate the execution of the same Turing machine starting from the same initial finite configuration. Of course, the whole initial configuration occurs in a big enough red triangle. If the configuration is not complete in a red triangle, the computation halts on the basis of the red triangle. Accordingly as the red triangles are bigger and bigger, if the machine does not stop, it is possible to tile the plane. If the machine halts, the halting produces a tile which prevents the tiling to be completed. As far as the halting problem of Turing machines starting from a finite initial configuration is undecidable, that reduction proves that the tiling problem of the hyperbolic plane is also undecidable.

As far as we know that there are enough active seeds, we have to look at how behave the triangles constructed from them.

The construction performed in Section 2 required the realization of the interwoven triangles starting from at least one wire as far as that alone entails the construction of bigger and bigger triangles which are disjoint from each other. To prove Theorem 1 we need that the computation is performed more or less similarly in the triangles of each wire. But that property is guaranteed by the synchronisation property of the silver and blue signals, as proved by Lemma 14.

3.4.1 The implementation

As can immediately be seen, the important feature is not that we have strictly parallel lines, and that squares are aligned along lines which are perpendicular to the tapes. What is important is that we have a **grid**, which may be a more or less distorted image of the just described representation.

We can reinforce Lemma 16:

Lemma 18 *For each tile τ , there is an active seed whose distance from τ is at most 12.*

Proof. In the worst case, assume that τ is a **B**-tile on an isocline m . The **O**-son of τ has a **Y**-son so, that at distance at most 4 there is a seed ρ say on the isocline n . As far as there are seeds on levels $n+4+k$ for any $k \in \mathbb{N}$, there is at least an active seen on some level $n+j$ with $j \leq 8$. Now, clearly, $n \leq m+4$. That proves the lemma. \square

On Figure 13, we can see two active seeds and several seeds which are not active. Accordingly, most seeds are not active but, the active ones are also dense in the heptagrid. It means that if we start to tile the heptagrid from an arbitrary tile, the blocking one being excepted, later or sooner we fall upon an active seed. We go back to that topic a bit later and also when we shall discuss the exact set of prototiles.

As already mentioned, the legs issued from an active seed σ follow the borders of $T(\sigma)$. Note that the active seeds also send signals on the green and the orange isoclines.

What is important is the thread-structure and Lemma 7. Note that the silver and the blue signals prevent the occurrence of two active seeds on the same isocline giving rise to trilaterals of different characteristics.

3.5 The tiles

In this sub-section, we shall describe as precisely as possible the tiles needed for the constructions defined in the previous sub-sections. The description is split into two parts.

We revisit the prototiles defined in Subsection 2.6 with Figures 14 and 15. Indeed, we have to implement the detection of the free rows, the construction of the red and of the blue signals and then the travel of the computing signal ξ . That latter is tightly connected with the program of the simulated Turing machine M so that the related prototiles should be better called **meta-tiles** as far as they bear variable signs for the content of a square of the tape of M , for the state of M and for the direction δ which has to be followed in order to meet the next **Y**-path. The detection of the free rows and the construction of red and blue signals are defined by Sub subsection 3.5.1. The management of the signal ξ is performed in Sub subsection 3.5.2.

3.5.1 The proto-tiles

With the silver signal, we fix the implementation of the triangles and of the phantom. The actual place of the generation $n+1$ is fixed by the first choice of an active seed which is in a free green isocline. If the active seed triggers a triangle, a phantom, the active seeds of the basis of the trilateral trigger a phantom, a triangle respectively. Whence the expected alternation which the whole construction is based upon.

The set of tiles we turn to now is called the set of **prototiles**. We subdivide the set into two parts: the construction of the isoclines and the construction of the trilaterals. A prototile is a pattern. Indeed, a tile is the indication of two data: the location of a tile in the heptagrid and the indication of a copy of the prototile which is placed at that location. The mark of the isoclines indicates which shifts are allowed: from a tile on an isocline to another tile on another isocline, provided that the marks of the image match with those of the new isocline.

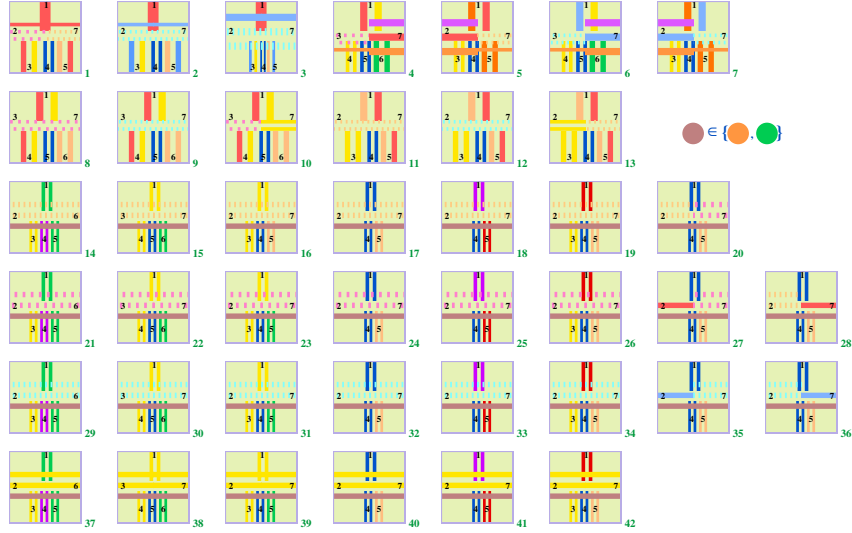


Figure 18 Generation of the red and the yellow signals by the legs of the triangle. Note that there are two red signals: one for the left-hand side legs and the other for the right-hand side ones. Taking into account the possible colours of the isocline, we get 75 tiles to be appended for those from Figures 14 and 15.

The set of prototiles forces the construction of the tiling with the isoclines. It also forces the activation of the seeds and the consecutive construction of the embedded triangles including the detection of the free rows in the triangles. We have already two figures to illustrate the prototiles: Figures 14 and 15. Each figure defines marks on the tiles for the construction of the tiling, of the isoclines, of the triangles and of the phantoms respectively. We append to those figures two new ones in order to introduce the new signals we defined: the red and the

yellow ones which allow us to locate the free rows.

Figure 18 illustrates the generation of the yellow and the red signals by the legs of a triangle. The figure makes use of meta-tiles in that meaning that the light mauve colour indicating the isocline can be freely replaced either by the orange colour or by the green one depending on which isocline we consider: remember that the red, blue and yellow signals run on green or orange isoclines only. Accordingly, that colour represents a variable for colours of the isoclines. A part of the tiles of Figure 18 are already present in Figure 15: the new red, blue or yellow signs are appended to those of Figure 15 for 20 of them.

Note that the tiles allowing red and blue signals to meet are attached to **B**-tiles: there are enough of them on each isocline. The distance between two consecutive **B**-tiles on an isocline is at most 5, as can be checked on Figure 13.

From that remark and summing the prototiles defined in Figures 14, 15 and 18, we get 232 prototiles.

Lemma 19 *There is a set of 232 prototiles which allow us to construct a tiling of the heptagrid implementing the embedded triangles with their isoclines together with the detection of the free rows in each triangle, the latitudes of trilaterals with identical attributes being synchronised.*

Note that the number of free rows in a trilateral is that of Lemma 13 as far as the basis of a triangle is not signalised as a free row.

In the appendix, several figures illustrate the construction of the tiling by focusing each one on one of the pictures belonging to Figure 9.

3.5.2 The meta-tiles

Let us now examine the construction of prototiles for simulating a Turing machine. As already mentioned, that part of the prototiles depends upon the Turing machine M which is simulated. It also depends on the data \mathcal{D} to which M is applied. Of course, it would be possible to consider Turing machines starting from an empty tape. The consequence would be a huge complexification of the machine which would store the data into its states. It is simpler to consider that M applies to a true data. It is the reason while we call these tiles **meta-tiles**.

As already mentioned, the simulation of the computation of M is organised in the red triangles, starting from generation 0. The interest of those infinitely many generations is the fact that as far as the number n of the generation increases, the number of free rows in the corresponding triangles also increases, which gives the tiling more time in the simulation of M . Also note that the space also increases as far as the height of a red triangle of the generation $2n+1$ is 8^{n+1} according to Lemma 7. As already mentioned, the initial configuration is displayed along the rightmost branch of a red triangle T which, outside the head of T , consists of **O**-tiles. A tree of the heptagrid rooted at a tile on the rightmost branch of T has its leftmost branch constituted of **Y**-tiles. Now, from Lemma 4, that borders does not meet the legs of a triangle inside T . Accordingly, the computation signal ξ travels on **Y**-tiles only when it goes from

a free row of T to the next one and it crosses consecutive tiles when it travels on a free row of T .

The meta-tiles are illustrated by Figure 19, where the caption explains the meaning of the colours.

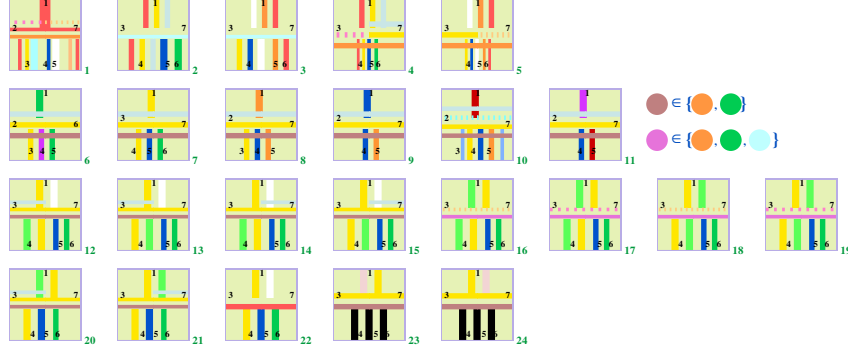


Figure 19 The meta-tiles for simulating the execution of the Turing machine M . Tile 1 represents the active seed for a triangle. Tiles 2 up to 5 allow the signals emitted for the computation to go down until the first orange or green isocline reached by tiles 3 and 4 for the left- and right-hand side legs respectively. Tiles 6 up to 11 allow the computing signal to travel on a free row of the triangle. Tiles 12 up to 15 illustrate the execution of an instruction. Tiles 16 up to 19 represent the crossing by the \mathbf{Y} -path of the isoclines covered by a red lateral signal. Tiles 20 and 21 illustrate the junction of the \mathbf{Y} -path with a free row, allowing the computing signal to go towards the next \mathbf{Y} -path. Tile 22 illustrates the case when the computing signal reaches the basis of the triangle which interrupts the computation. Tiles 23 and 24 indicate that the computation by the Turing machine halts. Those tiles are unique and cannot abut any other tile of the tiling.

A few supplementary explanations are needed.

Meta-tile 19.1 sends a white signal to the right-hand side leg of the triangle it generates. It triggers tile 19.3 which is on that leg in order to represent the squares of the Turing tape of M . Meta-tiles 19.6 up to 19.11 illustrate the travel of the current state of M on a free row. Note that if a seed occurs on that isocline, it must be active and it is either meta-tile 19.1 or 19.10 depending on whether the tile triggers a red triangle or a blue trilateral respectively. Meta-tiles 19.12 up to 19.15 illustrate the execution of an instruction: the current state travels on the free row going to left or to right, meta-tiles 19.14, 19.15 or 19.12, 19.13 respectively. The difference is seen on the \mathbf{Y} -son: if the new state goes to left, to right, the mark is put to left, to right respectively of the yellow mark of the \mathbf{Y} -son. Meta-tiles 19.16 up to 19.19 allow the new signal following the \mathbf{Y} -path to cross non free rows. When it reaches the free row, the new current states goes to left, to right, meta-tiles 19.20, 19.21 respectively depending on the side from which the current state came along the \mathbf{Y} -path. Meta-tile 19.22 is used when the current state reaches the basis of the red triangle: the computation is stopped as far as there is not enough free rows in that triangle for the computation of M .

Meta-tiles 19.23 and 19.24 are used when the current state is the halting state: when it meets the free row, the halting of the computation of M is implemented. Note that those latter tiles cannot abut any other tiles in those we defined and cannot abut each other or each one with itself. And so, we can see that the computation in a triangle always stops. Either it happens by the meeting of the computing signal along a **Y**-path with the basis of the triangle, or it happens by the halting of M itself. Meta-tiles 19.22 up to 19.24 illustrate those situations.

The number of meta-tiles depends upon the number s of states and the number ℓ of letters of M . From Figure 19, we can made the following counting:

- in Figure 19, tiles: 1 – 5: 5 tiles;
- 6 – 11: $12 \times \ell$ tiles: two possible isoclines and ℓ possible states;
- 12 – 15: $2 \times I$ tiles; I : number of instructions of M ;
- 16 – 19: $3 \times I$ tiles: the four tiles together, three possible isoclines and I_ℓ possible instructions;
- 20 – 21: $2 \times I$ tiles; two possible isoclines, I_ℓ possible instructions;
- 22 – 24: 3 tiles.

where I is the number of instructions of the program of M , ℓ is the number of states and s is the number of letters. Also D is the length of the data written with letters of M .

Accordingly, the total number of meta-tiles is $7.I + 12.\ell + D + 8$.

Combining that result with the previous countings we get:

Lemma 20 *For each Turing machine M with s states and ℓ letters whose program contains I instructions exactly, and whose data requires D letters, there is a set $\mathcal{P}_{M,D}$ of $240 + 7.I + 12.\ell + D$ prototiles, so that the tiling problem is undecidable for the set of all $\mathcal{P}_{M,D}$ applied to data written with letters of M .*

That completes the proof of Theorem 1.

4 A few corollaries for connected tiling problems

For the convenience of the reader, that section reproduces the similar section of [20].

The construction leading to the proof of Theorem 1 allows to get a few results in the same line of problems.

As indicated in [3, 4], there is a connection between the general tiling problem and the **Heesch number** of a tiling. That number is defined as the maximum number of **coronas** of a disc which can be formed with the tiles of a given set of tiles, see [8] for more information. As indicated in [4], and as our construction fits in the case of domino tilings, we have the following corollary of Theorem 1.

Theorem 3 *There is no computable function which bounds the Heesch number for the tilings of the hyperbolic plane.*

The construction of [12] gives the following result, see [13, 15].

Theorem 4 *The finite tiling problem is undecidable for the hyperbolic plane.*

Indeed, when the Turing machine halts, the halting state triggers a signal which encloses the computation area and which compels the tiling to be completed by blank tiles only, see [15].

Combining the construction proving Theorem 4 and the partition theorem which is proved in [16], chapter 4, section 4.5.2 about the splitting of Fibonacci patchworks, also see [11], the construction of this paper allows us to establish the following result, see [14].

Theorem 5 *The periodic tiling problem is undecidable for the hyperbolic plane, also in its domino version.*

Note that the analog of Theorem 5 for the Euclidean plane was proved by Gurevich and Koriakov, see [5].

In the statement of Theorem 5, **periodic** means that there is a shift which leaves the tiling globally invariant. The construction mimics that of Theorem 4 in the fact that if the simulated Turing machine halts, we also enclose the computing area. But this time, we enlarge the notion of computing area and of triangles so as to also permits black trees to support embedded triangles. In this way, we can define areas of the kind defined by Fibonacci patchworks and of the size dictated by the halting of the machine. We define colours for these surrounding signals in such a way that they entail a construction of a scaled Fibonacci tree, see [19]. Next, it is not difficult to construct a tiling of the hyperbolic plane in this way, periodically, applying the shifts already mentioned in [16], chapter 4, section 4.5.3, also see [11].

At last, in another direction, we may apply the arguments of Hanf and Myers, see [6, 21], and prove the following result.

Theorem 6 *There is a finite set of tiles such that it generates only non-recursive tilings of the hyperbolic plane.*

The proof makes use of the construction of two incomparable recursively enumerable sets A and B of integers. The set of tiles defines the computation of these sets by a Turing machine. Moreover, the set of tiles tiles the plane if and only if there is a set to separate A from B . As such a set cannot be constructed by an algorithm, we obtain the result stated in Theorem 6.

4.1 Conclusion

It seems to me that the construction of Section 2 could be applied to prove undecidability problems on cellular automata. Of course, the halting problem for cellular automata is undecidable, but this is a simple consequence of the undecidability of the same problem for Turing machines.

In fact, it is interesting to notice that the construction of Section 2 which is based on Construction 3 can be performed by a cellular automaton.

The working of the automaton could be devised as follows.

We consider that the automaton works on three layers. On the first one, it tries to construct the tiling. The initial configuration of this layer is a blank plane, except at a tile called central, which is an active seed. On the second layer, the cellular automaton updates a ball around the central tile which coincides with that of the first layer. The third layer is a ‘working sheet’ for intermediate computations performed by the automaton.

It is plain that if the Turing machine implemented in the set of tiles does not halt, the cellular automaton will tile the plane in infinite time. If the Turing machine halts, the cellular automaton will take notice that the construction is stopped at some point.

A last consequence of the construction of Section 2 leads us back to hyperbolic geometry.

We used Figure 12, in order to better understand Construction 3. It is worth noticing that both figures are indeed Euclidean constructions. However, Construction 3 proceeds in a hyperbolic tiling. It seems to me that the fact that this transfer is possible has an important meaning. From my humble point of view, it means that a construction which seems to be purely Euclidean has indeed a purely combinatoric character. It belongs to absolute geometry and it mainly requires Archimedes’ axiom. Note that absolute geometry itself has no pure model. A realisation is necessarily either Euclidean or hyperbolic. To conclude with it, we suggest that probably the extent of absolute geometry is somehow under-estimated.

As indicated in the Introduction, the construction of the paper is inspired by the construction of the paper I wrote in 2007 to prove Theorem 1. However, and it was the main goal of the present paper, the number of needed prototiles is significantly reduced.

From Lemma 20, simulating a Turing machine M whose program contains I instructions for s states and ℓ and which letters applied to a data \mathcal{D} of length D with a tiling, $240+7.I+12.\ell+D$ prototiles are needed in our simulation. In contrast, paper [20] required $556+20.I+136.s+12.\ell+D$ for the same goal while my 2007 paper [18] required $18870+880.s+1852.\ell+192.I+D$ prototiles. Note that the importance of the parameters involved in those formulas seriously depends on M and on its data. For the same Turing machine M there are infinitely many possible data so that D is the single variable. If we consider tiny universal Turing machines, see [22] for example, D is enormous in comparison with I . As far for a single Turing machine there are infinitely many possible data, it makes sense to focus our attention on the program of M . If we apply those formulas to the universal Turing machine with 6 states and 4 letters from [22] we get 449 prototiles with the present paper, while 1884 prototiles are required in [20] and 35782 of them for [18]. The present result is at least four times better than that of [20] and more than seventy nine times better than that of [18].

If we consider Turing machines with a high number of instructions and if we ignore the size of the data, then in the present paper the amount of prototiles is of order $7.I$, it is $12.I$ in [20] and $192.I$ in [18]. Accordingly, in magnitude, the

present paper is a bit more than 1.71 better than [20] and it divides by more than 27 that of [18].

Note that if we consider a fixed universal Turing machine U and if we consider the halting problem for U applied to all its possible data, that problem is also undecidable. If U is the considered tiny universal Turing machine, the single variable is then D . In that case, the previous formulas are all of the order of D .

References

- [1] Berger R., The undecidability of the domino problem, *Memoirs of the American Mathematical Society*, **66**, (1966), 1-72.
- [2] Chelghoum K., Margenstern M., Martin B., Pecci I., Cellular automata in the hyperbolic plane: proposal for a new environment, *Lecture Notes in Computer Sciences*, **3305**, (2004), 678-687, proceedings of ACRI'2004, Amsterdam, October, 25-27, 2004.
- [3] Goodman-Strauss, Ch., A strongly aperiodic set of tiles in the hyperbolic plane, *Inventiones Mathematicae*, **159**(1), (2005), 119-132.
- [4] Goodman-Strauss, Ch., Growth, aperiodicity and undecidability, *invited address at the AMS meeting at Davidson, NC*, March, 3-4, (2007).
- [5] Gurevich Yu., Koriakov I., A remark on Berger's paper on the domino problem, *Siberian Mathematical Journal*, **13**, (1972), 459-463.
- [6] Hanf W., Nonrecursive tilings of the plane. I. *Journal of Symbolic Logic*, **39**, (1974), 283-285.
- [7] Hopcroft, J.E., Motwani, R., Ullman, J.D., *Introduction to Automata Theory, Languages, and Computation*, Addison Wesley, Boston/San Francisco/New York, (2001).
- [8] Mann C., Heesch's tiling problem, *American Mathematical Monthly*, **111**(6), (2004), 509-517.
- [9] Margenstern M., New Tools for Cellular Automata of the Hyperbolic Plane, *Journal of Universal Computer Science* **6**N°12, 1226-1252, (2000)
- [10] Margenstern M., Cellular Automata and Combinatoric Tilings in Hyperbolic Spaces, a survey, *Lecture Notes in Computer Sciences*, **2731**, (2003), 48-72.
- [11] Margenstern M., A new way to implement cellular automata on the penta- and heptagrids, *Journal of Cellular Automata* **1**, N°1, (2006), 1-24.
- [12] Margenstern M., About the domino problem in the hyperbolic plane from an algorithmic point of view, *iarXiv:cs.CG/0603093 v1*, (2006), 11p.
- [13] Margenstern M., The finite tiling problem is undecidable in the hyperbolic plane, *arxiv:cs.CG/0703147v1*, (2007), March, 8p.

- [14] Margenstern M., The periodic domino problem is undecidable in the hyperbolic plane, *arxiv.cs.CG/0703153v1*, (2007), March, 12p.
- [15] Margenstern M., The Finite Tiling Problem Is Undecidable in the Hyperbolic Plane, *Workshop on Reachability Problems*, **RP07**, July 2007, Turku, Finland,
- [16] Margenstern M., Cellular Automata in Hyperbolic Spaces, Volume 1, Theory, *OCP*, Philadelphia, (2007), 422p.
- [17] Margenstern M., The Domino Problem of the Hyperbolic Plane is Undecidable, *Bulletin of the EATCS*, **93**, October, (2007), 220-237.
- [18] Margenstern M., The domino problem of the hyperbolic plane is undecidable, *Theoretical Computer Science*, **407**(1-3), (2008), 29-84.
- [19] Margenstern M., A Uniform and Intrinsic Proof that there are Universal Cellular Automata in Hyperbolic Spaces, *Journal of Cellular Automata* **3**, N°2, (2008), 157-180.
- [20] Margenstern M., The domino problem of the hyperbolic plane is undecidable, new proof, *arXiv.cs.DM/2205.07317v1*, (2022), May, 49pp.
- [21] Myers D., Nonrecursive tilings of the plane. II. *Journal of Symbolic Logic*, **39**, (1974), 286-294.
- [22] Neary T., Woods D., Four Small Universal Turing Machines, *Fundamenta Informaticae*, **91**(1), (2009), 123-144.
- [23] Robinson R.M. Undecidability and nonperiodicity for tilings of the plane, *Inventiones Mathematicae*, **12**, (1971), 177-209.
- [24] Robinson R.M. Undecidable tiling problems in the hyperbolic plane. *Inventiones Mathematicae*, **44**, (1978), 259-264.
- [25] Turing A.M., On computable real numbers, with an application to the Entscheidungsproblem, *Proceedings of the London Mathematical Society*, ser. 2, **42**, 230-265, (1936).
- [26] Wang H. Proving theorems by pattern recognition, Bell System Tech. J. vol. **40** (1961), 1-41.

Appendix

We first reproduce the pictures for the construction of the interwoven triangles at a larger scale.

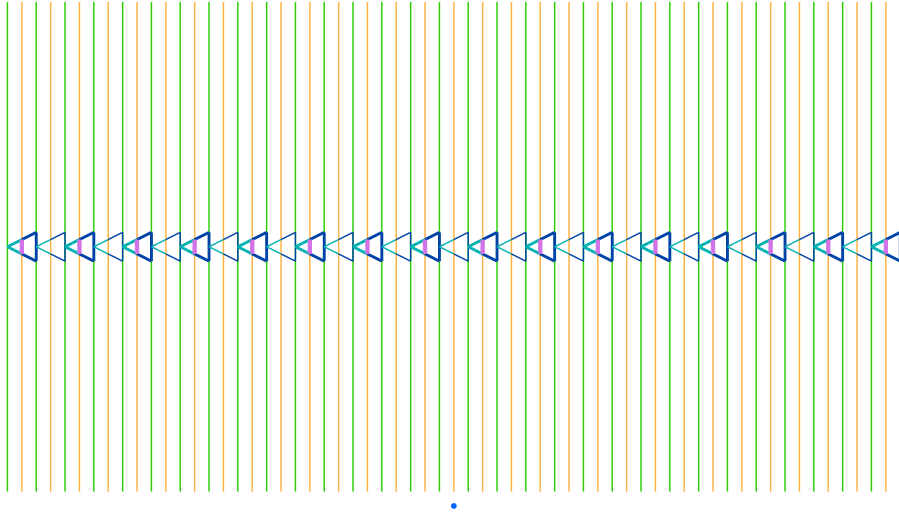


Figure 20 The isoclines and the generation 0 of the interwoven triangles. Note the alternation of triangles and phantoms.

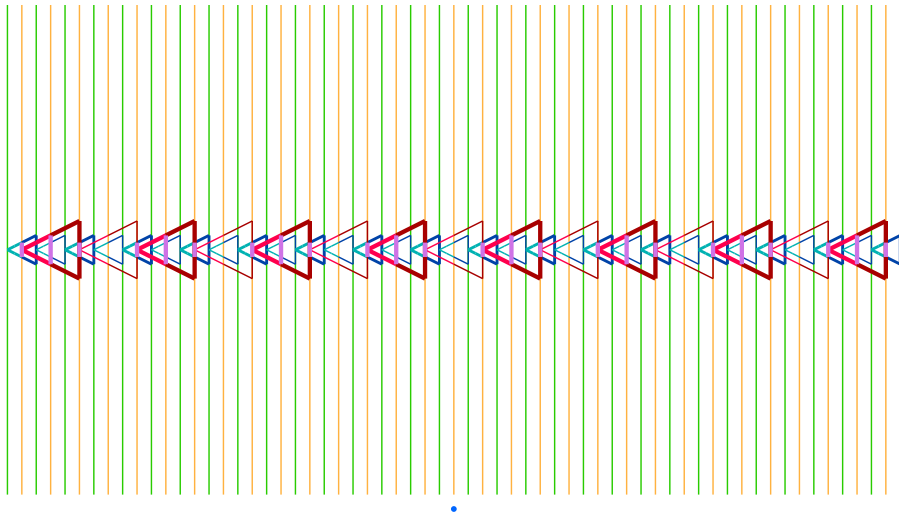


Figure 21 The isoclines and the generations 0 and 1 of the interwoven triangles. Note the alternation of triangles and phantoms of the same colour

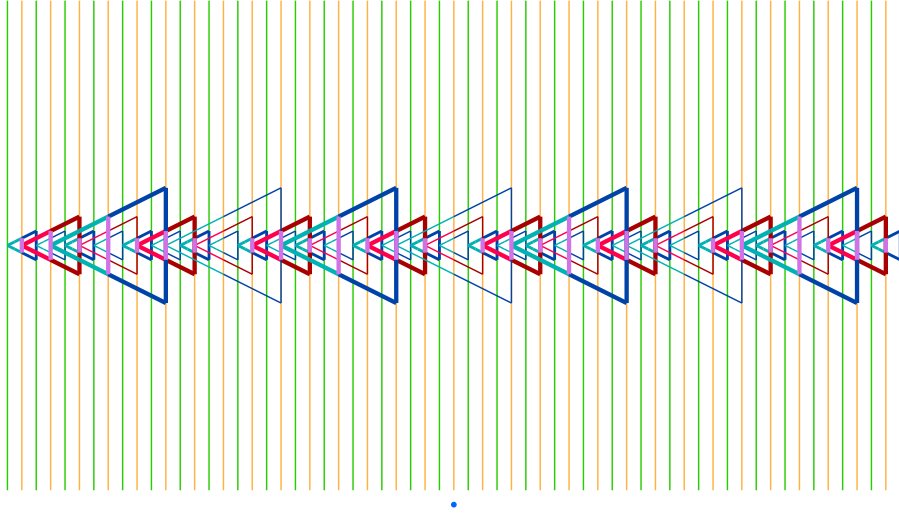


Figure 22 The isoclines and the generations 0, 1 and 2 of the interwoven triangles. Note the alternation of triangles and phantoms of the same colour

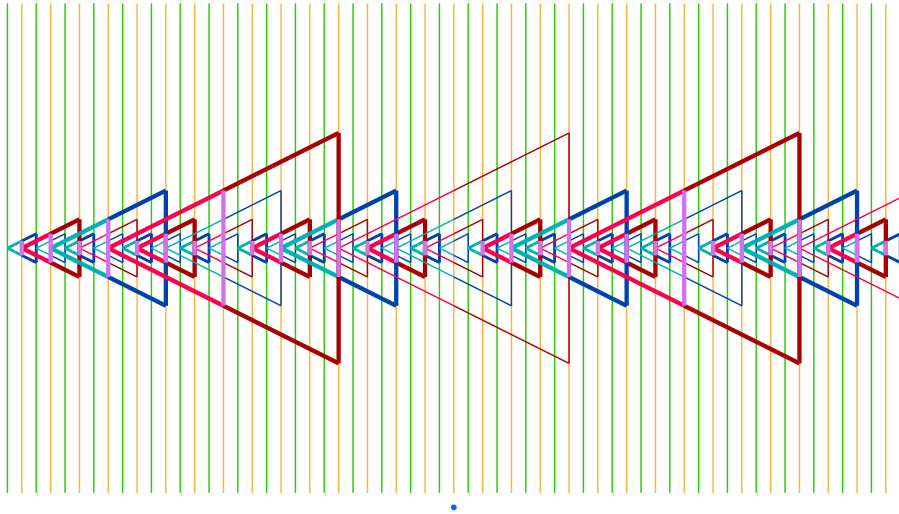


Figure 23 The isoclines and the generations 0, 1, 2 and 3 of the interwoven triangles. Note the alternation of triangles and phantoms of the same colour

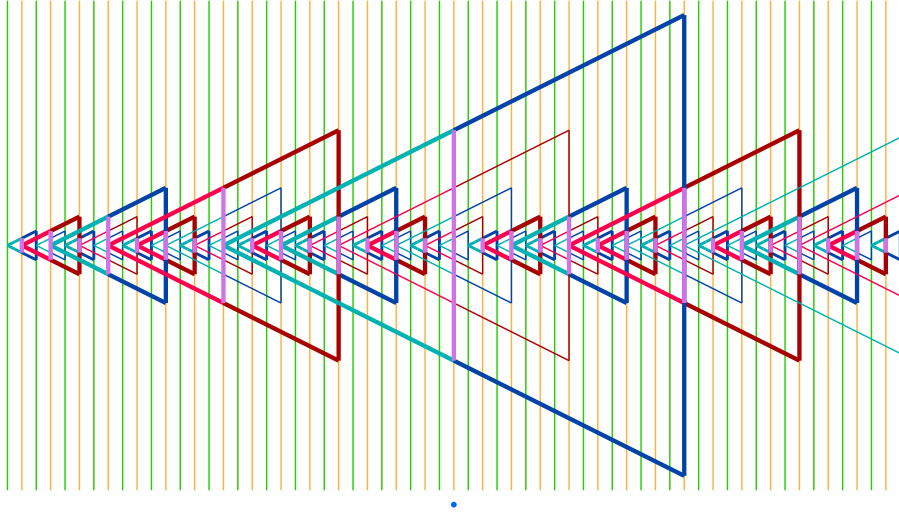


Figure 24 The isoclines and the generations 0, 1, 2, 3 and 4 of the interwoven triangles. Note the alternation of triangles and phantoms of the same colour

As announced in Subsection 2.5 we give several figures where the neighbourhood of the central tile occurs in Figure 9. Figure 26 illustrates how the rules are applicated starting from a fixed central and its father according to Figure 9. The following figures apply the same principle.

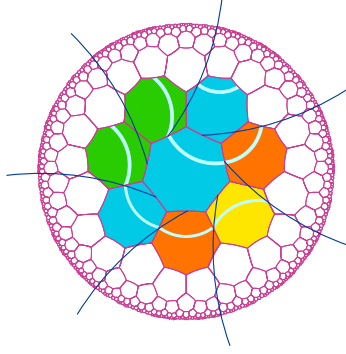


Figure 25 The central tile and its immediate neighbourhood is that of Figure 26.



Figure 26 Central tile: a **B**-tile whose father is also a **B**-tile. The rules of (R_1) are applied.

Presently, the **B**-tiles with, as father, an **O**-tile then a **Y**-one. There cannot be a **G**-father: in that case, the **B**-son is replaced by an **M**-one, see Figure 29

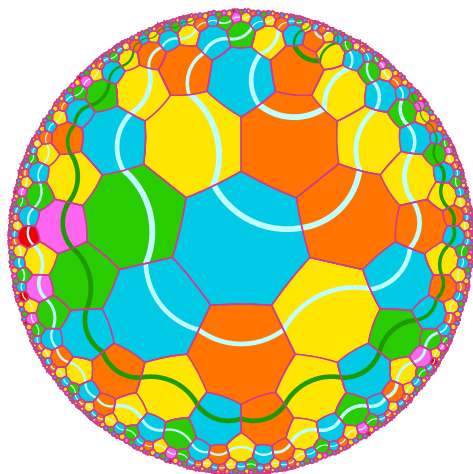


Figure 27 Central tile: a **B**-tile whose father is an **O**-tile. The rules of (R_1) are applied.

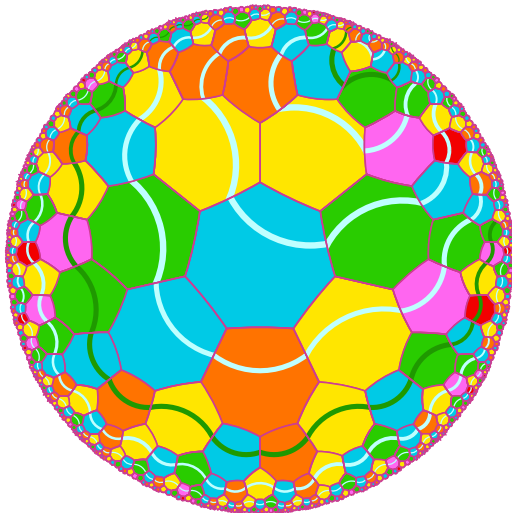


Figure 28 Central tile: a **B**-tile whose father is a **Y**-tile. The rules of (R_1) are applied.

Presently, the case of an **M**-tile whose father is necessarily a **G**-tile, according to rules (R_1) .

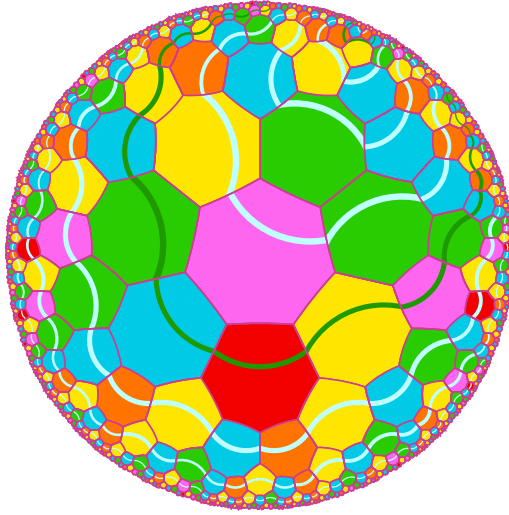


Figure 29 Central tile: an **M**-tile. Its father is necessarily a **G**-tile. The rules of (R_1) are applied. Note that the neighbourhood is different from those of Figures 26 and 27.

Presently, the central tile are **Y**-tiles in the four following figures.

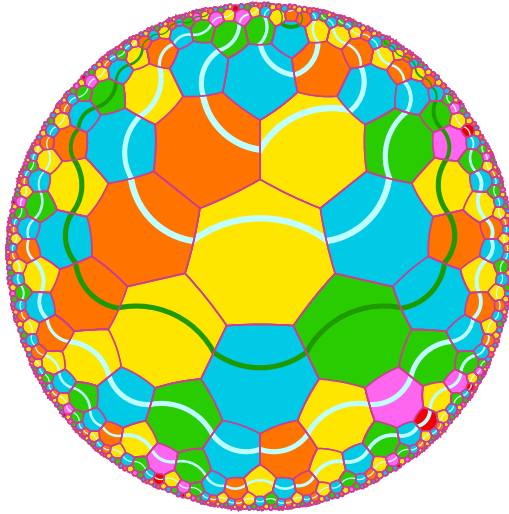


Figure 30 Central tile: a **Y**-tile whose father is also a **Y**-tile. The rules of (R_1) are applied.

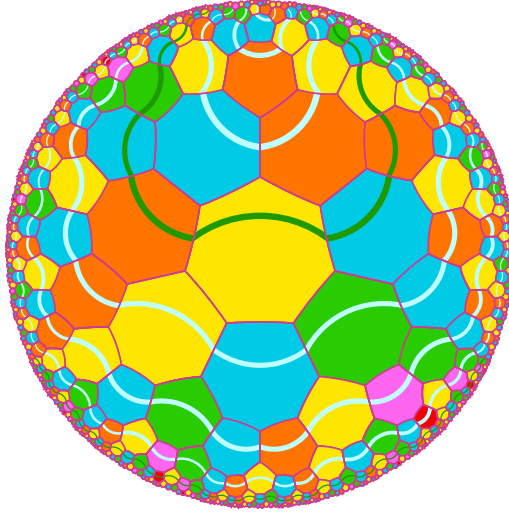


Figure 31 Central tile: a **Y**-tile whose father is an **O**-tile. The rules of (R_1) are applied. The neighbourhood is different from that of Figure 30.

In Figures 32 and 33, the father is a **G**-tile.

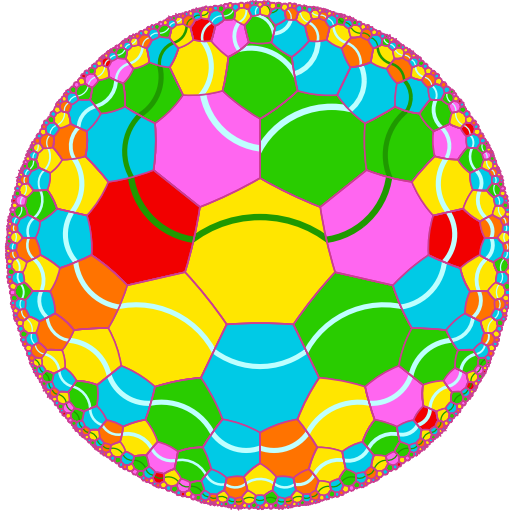


Figure 32 Central tile: a **Y**-tile whose father is a **G**-tile. The rules of (R_1) are applied. Neighbours 2 and 7 of the central tile are an **M**-tile.



Figure 33 Central tile: a **Y**-tile whose father is a **G**-tile. The rules of (R_1) are applied. Neighbour 2 of the central tile is a **B**-tile, neighbour 7 is an **M**-one.

Presently, the central tile is a **G**-tile. The father is either a **Y**-tile or a **G**-one.

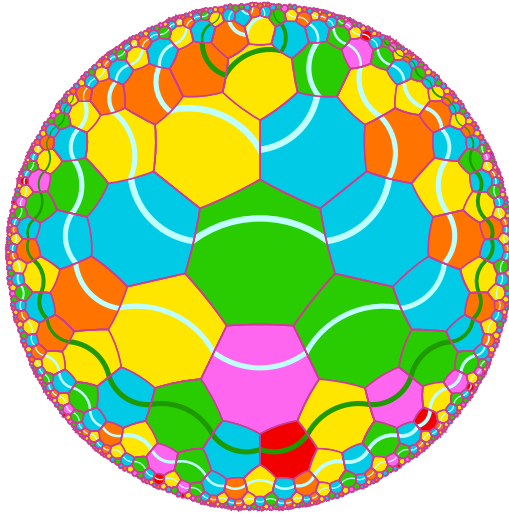


Figure 34 Central tile: a **G**-tile whose father is a **Y**-tile. The rules of (R_1) are applied. Neighbours 4 of the central tile is an **M**-tile. Neighbour 2 is a **B**-one.



Figure 35 Central tile: a **G**-tile whose father is also a **G**-tile. The rules of (R_1) are applied. Neighbour 2 of the central tile is a **B**-tile, neighbour 3 is an **M**-one.

Presently, the central tile is an **O**-tile. The father is either a **B**-tile or an **O**-one.

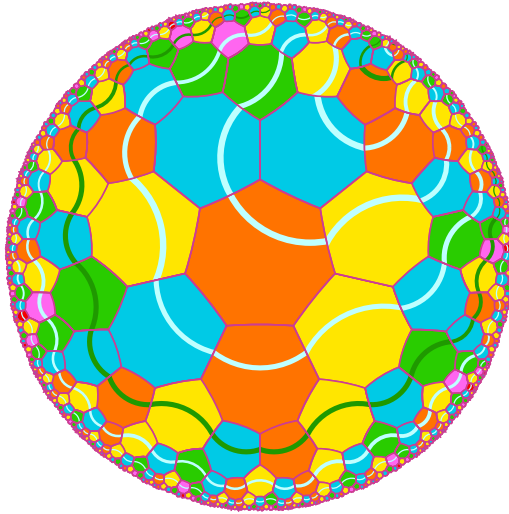


Figure 36 Central tile: an **O**-tile whose father is a **B**-tile. The rules of (R_1) are applied.

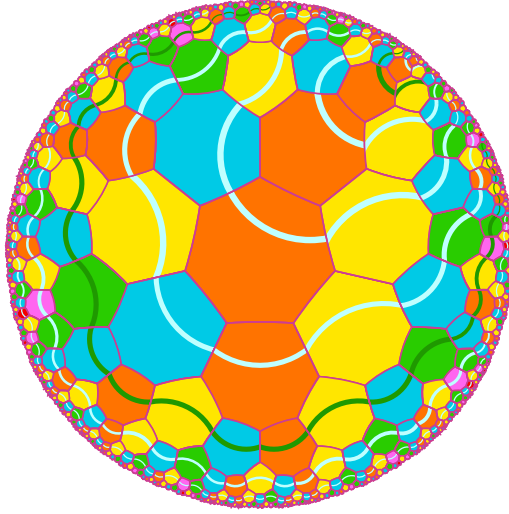


Figure 37 Central tile: an **O**-tile whose father is an **O**-tile. The rules of (R_1) are applied. Besides the father, the neighbourhood is the same as in Figure 36.

Presently, the central tile is an **R**-tile. The father is necessarily an **M**-tile.

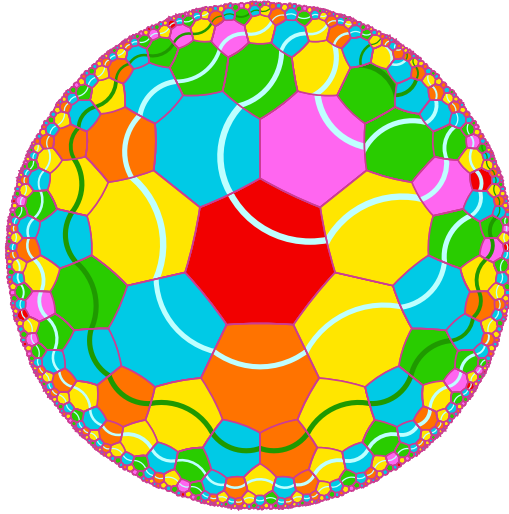


Figure 38 Central tile: an **R**-tile. The father is an **M**-tile. The rules of (R_1) are applied. The neighbourhood is different from those of Figures 36 and 37 despite the fact that the rules are similar to those involving **O**-tiles.